

Learning to be Global Optimizer

Haotian Zhang, Jianyong Sun and Zongben Xu

Abstract—The advancement of artificial intelligence has cast a new light on the development of optimization algorithm. This paper proposes to *learn* a two-phase (including a minimization phase and an escaping phase) global optimization algorithm for smooth non-convex functions. For the minimization phase, a model-driven deep learning method is developed to learn the update rule of descent direction, which is formalized as a non-linear combination of historical information, for convex functions. We prove that the resultant algorithm with the proposed adaptive direction guarantees convergence for convex functions. Empirical study shows that the learned algorithm significantly outperforms some well-known classical optimization algorithms, such as gradient descent, conjugate descent and BFGS, and performs well on ill-posed functions. The escaping phase from local optimum is modeled as a Markov decision process with a fixed escaping policy. We further propose to learn an optimal escaping policy by reinforcement learning. The effectiveness of the escaping policies is verified by optimizing synthesized functions and training a deep neural network for CIFAR image classification. The learned two-phase global optimization algorithm demonstrates a promising global search capability on some benchmark functions and machine learning tasks.

Index Terms—two-phase global optimization, learning to learn, model-driven deep learning, reinforcement learning, Markov Decision Process

I. INTRODUCTION

This paper considers unconstrained continuous global optimization problem:

$$\min_{\mathbf{x} \in \mathbb{R}^n} f(\mathbf{x}) \quad (1)$$

where f is smooth and non-convex. The study of continuous global optimization can be dated back to 1950s [1]. The outcomes are very fruitful, please see [2] for a basic reference on most aspects of global optimization, [3] for a comprehensive archive of online information, and [4] for practical applications.

Numerical methods for global optimization can be classified into four categories according to their available guarantees, namely, incomplete, asymptotically complete, complete, and rigorous methods [5]. We make no attempt on referencing or reviewing the large amount of literatures. Interested readers please refer to a WWW survey by Hart [6] and Neumaier [3]. Instead, this paper focuses on a sub-category of incomplete method, the two-phase approach [7], [8].

A two-phase optimization approach is composed of a sequence of cycles, each cycle consists of two phases, a minimization phase and an escaping phase. At the minimization phase, a minimization algorithm is used to find a local minimum for a given starting point. The escaping phase aims

to obtain a good starting point for the next minimization phase so that the point is able to escape from the local minimum.

A. The Minimization Phase

Classical line search iterative optimization algorithms, such as gradient descent, conjugate gradient descent, Newton method, and quasi-Newton methods like DFP and BFGS, etc., have flourished decades since 1940s [9], [10]. These algorithms can be readily used in the minimization phase.

At each iteration, these algorithms usually take the following location update formula:

$$x_{k+1} = x_k + \Delta_k \quad (2)$$

where k is the iteration index, x_{k+1}, x_k are the iterates, Δ_k is often taken as $\alpha_k \cdot d_k$ where α_k is the step size and d_k is the descent direction. It is the chosen of d_k that largely determines the performance of these algorithms in terms of convergence guarantees and rates.

In these algorithms, d_k is updated by using first-order or second-order derivatives. For examples, $d_k = -\nabla f(x_k)$ in gradient descent (GD), and $-\left[\nabla^2 f(x_k)\right]^{-1} \nabla f(x_k)$ in Newton method where $\nabla^2 f(x_k)$ is the Hessian matrix. These algorithms were usually with mathematical guarantee on their convergence for convex functions. Further, it has been proven that first-order methods such as gradient descent usually converges slowly (with linear convergence rate), while second-order methods such as conjugate gradient and quasi-Newton can be faster (with super linear convergence rate), but their numerical performances could be poor in some cases (e.g. quadratic programming with ill-conditioned Hessian due to poorly chosen initial points).

For a specific optimization problem, it is usually hard to tell which of these algorithms is more appropriate. Further, the no-free-lunch theorem [11] states that “for any algorithm, any elevated performance over one class of problems is offset by performance over another class”. In light of this theorem, efforts have been made on developing optimization algorithms with adaptive descent directions.

The study of combination of various descent directions can be found way back to 1960s. For examples, the Broyden family [12] uses a linear combination of DFP and BFGS updates for the approximation to the inverse Hessian. In the Levenberg-Marquardt (LM) algorithm [13] for nonlinear least square problem, a linear combination of the Hessian and identity matrix with non-negative damping factor is employed to avoid slow convergence in the direction of small gradients. In the accelerated gradient method and recently proposed stochastic optimization algorithms, such as momentum [14], AdaGrad [15], AdaDelta [16], ADAM [17] and such, moments of the first-order and second-order gradients are combined and estimated iteratively to obtain the location update.

HZ, JS and ZX are all with the School of Mathematics and Statistics and National Engineering Laboratory for Big Data Analytics, Xi'an Jiaotong University, Xi'an, China. Corresponding author: Jianyong Sun, email: jy.sun@xjtu.edu.cn

Besides these work, only recently the location update Δ_k is proposed to be adaptively *learned* by considering it as a parameterized function of appropriate historical information:

$$\Delta_k = g(S_k; \theta_k) \quad (3)$$

where S_k represents the information gathered up to k iterations, including such as iterates, gradients, function criteria, Hessians and so on, and θ_k is the parameter.

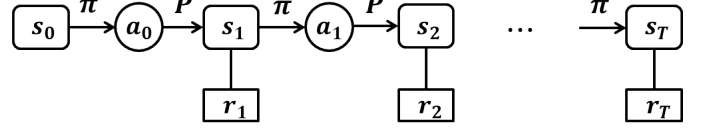
Neural networks are used to model $g(S_k; \theta_k)$ in recent literature simply because they are capable of approximating any smooth function. For example, Andrychowicz et al. [18] proposed to model d_k by long short term memory (LSTM) neural network [19] for differentiable f , in which the input of LSTM includes $\nabla f(x_k)$ and the hidden states of LSTM. Li et al. [20] used neural networks to model the location update for some machine learning tasks such as logistic/linear regression and neural net classifier. Chen et al. [21] proposed to obtain the iterate directly for black-box optimization problems, where the iterate is obtained by LSTM which take previous queries and function evaluations, and hidden states as inputs.

Neural networks used in existing learning to learn approaches are simply used as a block box. The interpretability issue of deep learning is thus inherited. A model-driven method with prior knowledge from hand-crafted classical optimization algorithms is thus much appealing. Model driven deep learning [22], [23] has shown its ability on learning hyper-parameters for a compressed sensing problem of the MRI image analysis, and for stochastic gradient descent methods [24], [25].

B. The Escaping Phase

A few methods, including tunneling [26] and filled function [8], have been proposed to escape from local optimum. The tunneling method was first proposed by Levy and Montalvo [26]. The core idea is to use the zero of an auxiliary function, called tunneling function, as the new starting point for next minimization phase. The filled function method was first proposed by Ge and Qin [8]. The method aims to find a point which falls into the attraction basin of a better than current local minimizer by minimizing an auxiliary function, called the filled function. The tunneling and filled function methods are all based on the construction of auxiliary function, and the auxiliary functions are all built upon the local minimum obtained from previous minimization phase. They are all originally proposed for smooth global optimization.

Existing research on tunneling and filled function is either on developing better auxiliary functions or extending to constrained and non-smooth optimization problems [27], [28], [29]. In general, these methods have similar drawbacks. First, the finding of zero or optimizer of the auxiliary function is itself a hard optimization problem. Second, it is not always guaranteed to find a better starting point when minimizing the auxiliary function [30]. Third, there often exists some hyper-parameters which are critical to the methods' escaping performances, but are difficult to control [31]. Fourth, some proposed auxiliary functions are built with exponent or logarithm term. This could cause ill-condition problem for the



s_{t+1} conditionally based on s_t and a_t . The policy $\pi : \mathcal{S} \times \mathcal{A} \times \{0, 1, \dots, T\} \rightarrow \mathbb{R}$, where $\pi(a_t|s_t; \theta)$ is the probability of choosing action a_t when observing current state s_t with θ as the parameter.

As shown in Fig. 1, starting from a state $s_0 \sim \mu_0$, the agent chooses $a_0 \sim \pi(a_0|s_0, \theta)$; after executing the action, agent arrives at state $s_1 \sim p(s_1|a_0, s_0)$. Meanwhile, agent receives a reward $r(s_1)$ (or r_1) from the environment. Iteratively, a trajectory $\tau = \{s_0, a_0, r_1, s_1, a_1, r_2, \dots, a_{T-1}, s_T, r_T\}$ can be obtained. The optimal policy π^* is to be found by maximizing the expectation of the cumulative reward $R(\tau) = \left[\sum_{t=0}^{T-1} \gamma^t r(s_{t+1}) \right]$:

$$\pi^* = \arg \max_{\pi} \mathbb{E}_{\tau} [R_{\tau}] = \sum_{\tau} q(\tau; \theta) R(\tau) \triangleq U(\theta) \quad (4)$$

where the expectation is taken over trajectory $\tau \sim q(\tau; \theta)$ where

$$q(\tau; \theta) = \mu_0(s_0) \prod_{t=0}^{T-1} \pi(a_t|s_t, \theta) p(s_{t+1}|a_t, s_t). \quad (5)$$

A variety of reinforcement learning algorithms have been proposed for different scenarios of the state and action spaces, please see [32] for recent advancements. The RL algorithms have succeeded overwhelmingly for playing games such as GO [33], Atari [34] and many others.

We briefly introduce the policy gradient method for continuous state space [35], which will be used in our study. Taking derivative of $U(\theta)$ w.r.t. θ discarding unrelated terms, we have

$$\begin{aligned} \nabla U(\theta) &= \sum_{\tau} R(\tau) \nabla_{\theta} q(\tau; \theta) \\ &= \sum_{\tau} R(\tau) \nabla_{\theta} \log q(\tau; \theta) q(\tau; \theta) \\ &= \sum_{\tau} R(\tau) q(\tau; \theta) \left[\sum_{t=0}^{T-1} \nabla_{\theta} \log \pi(a_t|s_t, \theta) \right] \end{aligned} \quad (6)$$

Eq. 6 can be calculated by sampling trajectories τ_1, \dots, τ_N in practice:

$$\nabla U(\theta) \approx \frac{1}{N} \sum_{i=1}^N \sum_{t=0}^{T-1} \nabla_{\theta} \log \pi(a_t^{(i)}|s_t^{(i)}, \theta) R(\tau^i) \quad (7)$$

where $a_t^{(i)}(s_t^{(i)})$ denotes action (state) at time t in the i th trajectory, $R(\tau^i)$ is the cumulative reward of the i th trajectory.

For continuous state and action space, normally assume

$$\pi(a|s, \theta) = \frac{1}{\sqrt{2\pi}\sigma} \exp \left\{ -\frac{(a - \phi(s; \theta))^2}{\sigma^2} \right\} \quad (8)$$

where ϕ can be any smooth function, like radial basis function, linear function, and even neural networks.

III. MODEL-DRIVEN LEARNING TO LEARN FOR LOCAL SEARCH

In this section, we first summarize some well-known first- and second-order classical optimization algorithms. Then the proposed model-driven learning to optimize method for locally convex functions is presented.

A. Classical Optimization Methods

In the sequel, denote $g_k = \nabla f(x_k)$, $s_k = x_{k+1} - x_k$, $y_k = g_{k+1} - g_k$. The descent direction d_k at the k -th iteration of some classical methods is of the following form [12]:

$$d_k = \begin{cases} -g_k & \text{steepest GD} \\ -g_k + \alpha_k d_{k-1} & \text{conjugate GD} \\ -H_k g_k & \text{quasi-Newton} \end{cases} \quad (9)$$

where H_k is an approximation to the inverse of the Hessian matrix, and α_k is a coefficient that varies for different conjugate GDs. For example, α_k could take $g_k^T y_{k-1} / d_{k-1}^T y_{k-1}$ for Crowder-Wolfe conjugate gradient method [12].

The update of H_k also varies for different quasi-Newton methods. In the Huang family, H_k is updated as follows:

$$H_k = H_{k-1} + s_{k-1} u_{k-1}^T + H_{k-1} y_{k-1} v_{k-1}^T \quad (10)$$

where

$$u_{k-1} = a_{11} s_{k-1} + a_{12} H_{k-1}^T y_{k-1} \quad (11)$$

$$v_{k-1} = a_{21} s_{k-1} + a_{22} H_{k-1}^T y_{k-1} \quad (12)$$

$$u_{k-1}^T y_{k-1} = \rho, v_{k-1}^T y_{k-1} = -1 \quad (13)$$

The Broyden family is a special case of the Huang family in case $\rho = 1$, and $a_{12} = a_{21}$.

B. Learning the descent direction: d-Net

We propose to consider the descent direction d_k as a nonlinear function of $S_k = \{g_k, g_{k-1}, s_{k-1}, s_{k-2}, y_{k-2}\}$ with parameter $\theta_k = \{w_k^1, w_k^2, w_k^3, w_k^4, \beta_k\}$ for the adaptive computation of descent search direction $d_k = h(S_k; \theta_k)$. Denote

$$R_{k-1} = \mathbf{I} - \frac{s_{k-1}(w_k^1 g_k - w_k^2 g_{k-1})^T}{s_{k-1}^T (w_k^3 g_k - w_k^4 g_{k-1})}. \quad (14)$$

We propose

$$h(S_k; \theta_k) = -R_{k-1} (\beta_k H_{k-1} + (1 - \beta_k) \mathbf{I}) g_k \quad (15)$$

where \mathbf{I} is the identity matrix.

At each iteration, rather than updating H_{k-1} directly, we update the multiplication of R_{k-1} and H_{k-1} like in the Huang family [12]:

$$R_{k-1} H_{k-1} = R_{k-1} R_{k-2} H_{k-2} + \rho R_{k-1} \frac{s_{k-2} s_{k-2}^T}{s_{k-2}^T y_{k-2}}. \quad (16)$$

It can be seen that with different parameter w_k^i , $i = 1, \dots, 4$ and β_k settings, d_k can degenerate to different directions:

- when $w_k^1, w_k^2, w_k^3, w_k^4 \in \{0, 1\}$, the denominator of R_k is not zero, and $\beta_k = 0$, the update degenerates to conjugate gradient.
- when $w_k^1, w_k^2, w_k^3, w_k^4 \in \{0, 1\}$, and the denominator of R_k is not zero, and $\beta_k = 1$, the update becomes the preconditioned conjugate gradient.
- when $w_k^1 = 1, w_k^2 = 1, w_k^3 = 1, w_k^4 = 1$, and $\beta_k = 1$, the update degenerates to the Huang family.
- when $w_k^1 = 0, w_k^2 = 0$, the denominator of R_k is not zero, and $\beta_k = 0$ the update becomes the steepest GD.

Based on Eq. 15, a new optimization algorithm, called adaptive gradient descent algorithm (AGD), can be established.

It is summarized in Alg. 1. It is seen that to obtain a new direction by Eq. 15, information from two steps ahead is required as included in S_k . To initiate the computation of new direction, in Alg. 1, first a steep gradient descent step (lines 3-5) and then a non-linear descent step (lines 7-10) are applied. With these prepared information, AGD iterates (lines 14-18) until the norm of gradient at the solution x_k is less than a positive number ϵ .

Algorithm 1 The adaptive gradient descent algorithm (AGD)

- 1: initialize $x_0, H_0 \leftarrow I$ and $\epsilon > 0$;
- 2: # a steep gradient descent step
- 3: $g_0 \leftarrow \nabla f(x_0), d_0 \leftarrow g_0$
- 4: Choose α_0 through line search;
- 5: $x_1 \leftarrow x_0 - \alpha_0 g_0$;
- 6: # a non-linear descent step
- 7: $g_1 \leftarrow \nabla f(x_1), s_0 \leftarrow x_1 - x_0$;
- 8: Compute $R_0 \leftarrow I - \frac{s_0(w_1^T g_1 - w_1^T g_0)^T}{s_0^T(w_1^T g_1 - w_1^T g_0)}$ and $d_1 \leftarrow R_0 H_0 g_1$;
- 9: Choose α_1 through line search;
- 10: $x_2 \leftarrow x_1 - \alpha_1 d_1$;
- 11: Set $k \leftarrow 2$;
- 12: **repeat**
- 13: Compute $g_k \leftarrow \nabla f(x_k), s_{k-1} \leftarrow x_k - x_{k-1}, y_{k-2} \leftarrow g_{k-1} - g_{k-2}$;
- 14: Gather $S_k \leftarrow \{g_k, g_{k-1}, s_{k-1}, s_{k-2}, y_{k-2}\}$;
- 15: Compute $d_k \leftarrow h(S_k; \theta_k)$;
- 16: Choose α_k through line search;
- 17: Update $R_k H_k$;
- 18: $x_{k+1} \leftarrow x_k - \alpha_k d_k$;
- 19: $k \leftarrow k + 1$;
- 20: **until** $\|g_k\| \leq \epsilon$

To specify the parameters θ_k in the direction update function h , like [18], we unfold AGD into T iterations. Each iteration can be considered as a layer in a neural network. We thus have a ‘deep’ neural network with T layers. The resultant network is called *d-Net*. Fig. 2 shows the unfolding.

Like normal neural networks, we need to train for its parameters $\theta = \{\theta_1, \dots, \theta_T\}$. To learn the parameters, the loss function $\ell(\theta)$ is defined as

$$\begin{aligned} L(\theta) &= \mathbb{E}_{f \in \mathcal{F}} \left(\sum_{t=1}^T f(x_t) \right) \\ &= \mathbb{E}_{f \in \mathcal{F}} \left(\sum_{t=2}^T f(x_{t-1} + \alpha_t h(S_{t-1}; \theta_{t-1})) \right) \end{aligned} \quad (17)$$

That is, we expect these parameters are optimal not only to a single function, but to a class of functions \mathcal{F} ; and to all the criteria along the T iterations.

We hereby choose \mathcal{F} to be the Gaussian function family:

$$\mathcal{F}_G = \{f | f(x) = \exp(-x^T \Sigma^{-1} x), \Sigma \succeq 0, x \in \mathbb{R}^n\} \quad (18)$$

There are two reasons to choose the Gaussian function family. First, any $f \in \mathcal{F}_G$ is locally convex. That is, let $H(x)$ represents the Hessian matrix of $f(x)$, it is seen that

$$\lim_{x \rightarrow 0} H(x) = f(x) \Sigma^{-1} + \Sigma^{-1} x x^T f(x) = \Sigma^{-1} \succeq 0$$

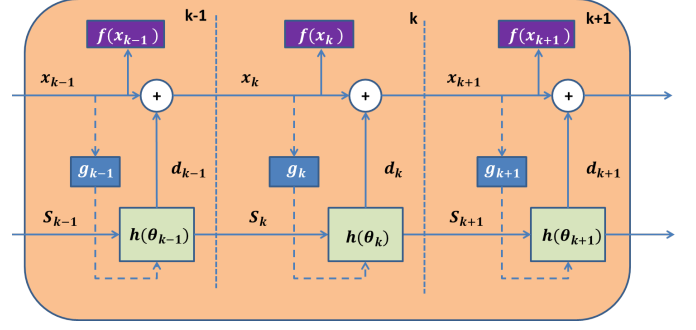


Fig. 2. The unfolding of the AGD.

Second, it is known that finite mixture Gaussian model can approximate a Riemann integrable function with arbitrary accuracy [36]. Therefore, to learn an optimization algorithm that guarantees convergence to local optima, it is sufficient to choose functions that are locally convex.

Given \mathcal{F} , when optimizing $\ell(\theta)$, the expectation can be obtained by Monte Carlo approximation with a set of functions sampled from \mathcal{F} , that is

$$\ell(\theta) \approx \frac{1}{N} \sum_{i=1}^N \sum_{t=2}^T f_i(x_{t-1} + \alpha_t h(S_{t-1}; \theta_{t-1}))$$

where $f_i \sim \mathcal{F}$. $\ell(\theta)$ can then be optimized by the steepest GD algorithm.

Note: The contribution of the proposed d-Net can be summarized as follows. First, there is a significant difference between the proposed learning to learn approach with existing methods, such as [18], [21]. In existing methods, LSTM is used as a ‘black-box’ for the determination of descent direction, and the parameters of the used LSTM is shared among the time horizon. Whereas in our approach, the direction is a combination of known and well-studied directions, i.e. a ‘white-box’, which means that our model is interpretable. This is a clear advantage against black-box models.

Second, in classical methods, such as the Broyden and Huang family and LM, descent directions are constructed through a linear combination. On the contrary, the proposed method is nonlinear and subsumes a wide range of classical methods. This may result in better directions.

Further, the combination parameters used in classical methods are considered to be hyper-parameters. They are normally set by trial and error. In the AGD, these parameters are learned from the optimization experiences to a class of functions, so that the directions can adapt to new optimization problem.

C. Group d-Net

To further improve the search ability of d-Net, we employ a group of d-Nets, dubbed as Gd-Net. These d-Nets are connected sequentially, with shared parameters among them. Input of the k -th ($k > 1$) d-Net is the gradient from $(k-1)$ -th d-Net. To apply Gd-Net, an initial point is taken as the input, and is brought forward through these d-Nets until the absolute gradient norm is less than a predefined small positive real number.

In the following we show that Gd-Net guarantees convergence to optimum for convex functions. We first prove that AGD is convergent. Theorem 1 summarizes the result. Please see Appendix A for proof.

Theorem 1. Assume $f : \mathbb{R}^n \rightarrow \mathbb{R}$ is continuous and differentiable and the sublevel set

$$L(x) = \{x \in \mathbb{R}^n | f(x) \leq f(x_0)\} \text{ for any } x_0 \in \mathbb{R}^n$$

is bounded. The sequence $\{x_k, k = 1, 2, \dots\}$ obtained by AGD with exact line search converges to a stable point.

Since d-Net is the unfolding of AGD, from Theorem 1, it is sure that the iterate sequence obtained by d-Net is non-increasing for any initial x_0 with properly learned parameters. Therefore, applying a sequence of d-Net (i.e. Gd-Net) on a bound function $f(x)$ from any initial point x_0 will result in a sequence of non-increasing function values. This ensures that the convergence of the sequence, which indicates that Gd-Net is convergent under the assumption of Theorem 1.

IV. ESCAPING FROM LOCAL OPTIMUM

Gd-Net guarantees convergence for locally convex functions. To approach global optimality, we present a method to escape from the local optimum once trapped. Our method is based on the filled-function method, and is embedded within the MDP framework.

A. The Escaping Phase in the Filled Function Method

In the escaping phase of the filled function method, a local search method is applied to minimize the filled function for a good starting point for next minimization phase. To apply the local search method, the starting point is set as $x_0 + \delta_0 d$ where x_0 is the local minimizer obtained from previous minimization phase, δ_0 is a small constant and d is the search direction.

Many filled functions have been constructed (please see [30] for a survey). One of the popular filled-functions [8] is defined as follows

$$H(x) = -\exp(a\|x - x_0\|^2)(f(x) - f(x_0)) \quad (19)$$

where a is a hyper-parameter. It is expected that minimizing $H(x)$ can lead to a local minimizer which is away from x_0 due to the exist of the exponential term.

Theoretical analysis has been conducted on the filled function methods in terms of its escaping ability [8]. However, the filled function methods have many practical weaknesses yet to overcome.

First, the hyper-parameter a is critical to algorithm performance. Basically speaking, if a is small, it struggles to escape from x_0 , otherwise it may miss some local minima. But it is very hard to determine the optimal value of a . There has no theoretical results, neither rule of thumb on how to choose a .

Second, the search direction d is also very important to the algorithmic performance. Different d 's may lead to different local minimizers, and the local minimizers are not necessarily better than x_0 . In literature, usually a trial-and-error procedure is applied to find the best direction from a set of pre-fixed

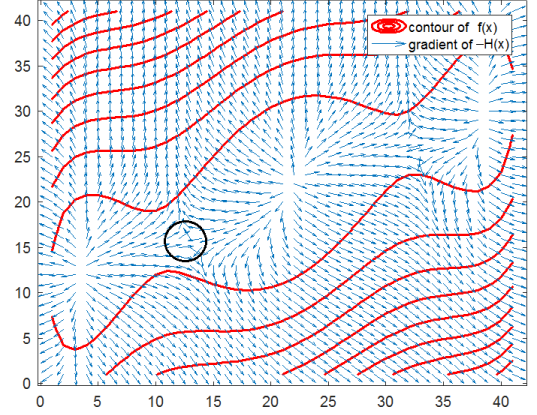


Fig. 3. Red lines show the contour of the three-hump function $f(x_1, x_2)$, blue arrows are the gradients of $-H(x_1, x_2)$. There is a saddle point at (12,15) for $-H(x_1, x_2)$.

directions, e.g. along the coordinates [8]. This is apparently not effective. To the best of our knowledge, no work has been done in this avenue.

Third, minimizing $H(x)$ itself is hard and may not lead to a local optimum, but a saddle point [8] even when a promising search direction is used. Unfortunately, there is no studies on how to deal with this scenario in literature. Fig. 3 shows a demo about this phenomenon. In the figure, the contour of $f(x)$ is shown in red lines, while the negative gradients of the filled function $H(x)$ are shown in blue arrows. From Fig. 3, it is seen that minimizing $H(x)$ from a local minimizer of f at (4, 13) will lead to the saddle point at (12, 15).

B. The Proposed Escaping Scheme

The goal of an escaping phase is to find a new starting point $x^{\text{new}} = x^{\text{old}} + \Delta x$ such that x^{new} can escape from the attraction basin of x^{old} (the local minimizer obtained from previous minimization phase) if a minimization procedure is applied, where $\Delta x = \delta d$, d is the direction and δ is called the escaping length in this paper.

Rather than choosing d from a pre-fixed set, we could sample some directions, either randomly or sequentially following certain rules. In this section, we propose an effective way to sample directions, or more precisely speaking Δx 's.

In our approach, the sampling of Δx is modeled as a finite-horizon MDP. That is, the sampling is viewed as the execution of a policy π : at each time step t , given the current state s_t , and reward r_{t+1} , an action a_t , i.e. the increment Δx , is obtained by the policy. The policy returns Δx by deciding a search direction d_t and an escaping length δ_t .

At each time step t , the state s_t is composed of a collection of previously used search directions $\mathbf{d}_t = \{d_1, \dots, d_{N_0}\}$ and their scores $\mathbf{u}_t = \{u_1, \dots, u_{N_0}\}$, where N_0 is a hyper-parameter. Here the score of a search direction measures how promising a direction is in terms of the quality of the new starting point that it can lead to. A new starting point is of high quality if applying local search from it can lead to a better minimizer than current one. The initial state s_0 includes

a set of N_0 directions sampled uniformly at random, and their corresponding scores.

In the following, we first define ‘score’, then present the policy on deciding a_t and δ_t , and the transition probability $p(s_{t+1}|a_t, s_t)$. Without causing confusion, we omit the subscript in the sequel.

1) *Score*: Given a search direction d , a local minimizer x_0 , define

$$u_d(t) = -\nabla f(x_0 + t \cdot d)^\top d \quad (20)$$

where $t \in \mathbb{R}_{++}$ is the step size along d .

Since x_0 is a local minimizer, by definition, we cannot find a solution with smaller f along d if $x_0 + td$ is within the attraction basin of x_0 . However, if there is a T such that $x' = x_0 + T \cdot d$ is a point with smaller criterion than x_0 (i.e. $f(x') < f(x_0)$), and there is no other local minimizer within $\mathcal{B}_0 = \{x \in \mathbb{R}^n | \|x - x_0\|_2 \leq \|x' - x_0\|_2\}$, we can prove that there exists a ξ , such that $u_d(t) < 0$ when $t \in [0, \xi]$, and $u_d(t) > 0$ when $t \in (\xi, T]$ (proof can be seen in Appendix B). Theorem 2 summarizes the result under the following assumptions:

- (1) $f(x) \in C^2(\mathbb{R}^n)$ has finite number of local minimizer.
- (2) For every local optimum x_ℓ , there exists a r such that $f(x)$ is convex in $\mathcal{B}(x_\ell, r) = \{x : \|x - x_\ell\|_2 \leq r\}$.
- (3) The attractive basin of each local optimum is convex.

Theorem 2. *If $x' = x_0 + T \cdot d$ is a point outside the boundary of x_0 's attraction basin, there is no other local minimizer within $\mathcal{B}_0 = \{x \in \mathbb{R}^n | \|x - x_0\|_2 \leq \|x' - x_0\|_2\}$. Then there exists a ξ such that*

$$g(t) \triangleq f(x_0 + t \cdot d), t \in [0, T]$$

obtains its maximum at ξ . And $g(t)$ is monotonically increasing in $[0, \xi]$, and monotonically decreasing in $(\xi, T]$.

If we let $d = x' - x_0$, then $g'(t) = \nabla f(x_0 + t(x' - x_0))^\top (x' - x_0) \triangleq -u_d(t)$. This implies that $u_d(t)$ is actually $-g'(t)$ along the direction from x' pointing to x_0 . This tells whether a direction d can lead to a new minimizer or not. A direction d with a positive $u_d(t)$ indicates that it could lead to a local minimizer different to present one.

We therefore define the score of a direction d , u_d , to be the greatest $u_d(t)$ along d , i.e.

$$u_d \triangleq \max_{t \in [0, T]} u_d(t) \quad (21)$$

For such d that $u_d > 0$, we say it is promising.

In the following, we present the policy π on finding Δx (or new starting point). The policy includes two sub-policies. One is to find the new point given a promising direction, i.e. to find the escaping length. The other is to decide the promising direction.

2) *Policy on finding the escaping length*: First we propose to use a simple filled function as follows:

$$\tilde{H}(x) = -a\|x - x_0\|^2. \quad (22)$$

Here a is called the ‘escaping length controller’ since it controls how far a solution could escape from the current local optimum. Alg. 2 summarizes the policy proposed to determine the optimal a^* and the new starting point x .

Algorithm 2 Policy on finding a new starting point

Require: a local minimum x_0 , a direction d , a bound $M > 0$, an initial escaping length controller $a > 0$, a learning rate α , some constants $\delta_0 > 0$, $N \in \mathbb{Z}$ and $\epsilon > 0$

Ensure: a new starting point x and u_d (the score of d)

- 1: **repeat**
 - 2: set $x_1 = x_0 + \delta_0 d$;
 - 3: optimize $\tilde{H}(x)$ along d starting from x_1 for N iterations, i.e. evaluate the criteria of a sequence of N points defined by $x_j = x_{j-1} + \alpha 2a(x_{j-1} - x_0)$, $2 \leq j \leq N$;
 - 4: compute $F(a) \leftarrow \sum_{j=2}^N f(x_j)/(j-1)$;
 - 5: $a \leftarrow a + \alpha F'(a)$;
 - 6: **until** $|F'(a)| \leq \epsilon$ or $\|x_N - x_0\| \geq M$.
 - 7: $u_d \leftarrow \max_{i=1, \dots, N} -\nabla f(x_i)^\top d$;
 - 8: **if** $\|x_N - x_0\| \geq M$, **then** set $u_d \leftarrow -|u_d|$;
 - 9: **return** u_d and $x \leftarrow x_N$.
-

In Alg. 2, given a direction d , the filled function $\tilde{H}(x)$ is optimized for N steps (line 3). The sum of the iterates’ function values, denoted as $F(a)$ (line 4), is maximized w.r.t. a by gradient ascent (line 5). The algorithm terminates if a stable point of $F(a)$ is found ($|F'(a)| \leq \epsilon$), or the search is out of bound ($\|x_N - x_0\| \geq M$). When the search is out of bound, a negative score is set for the direction d (line 8). As a by-product, Alg. 2 also returns the score u_d of the given direction d .

We prove that x_N can escape from the attraction basin of x_0 and ends up in another attraction basin of a local minimizer x' with smaller criterion if x' exists. Theorem 3 summarizes the result.

Theorem 3. *Suppose that $x' = x_0 + Td$ is a point such that $f(x_0) \geq f(x')$, and there are no other points that are with smaller or equal criterion than $f(x_0)$ within \mathcal{B}_0 . If the learning rate α is sufficiently small, then there exists an a^* such that $F'(a^*) = 0$.*

According to this theorem, we have the following corollary.

Corollary 1. *Suppose that x_N is the solution obtained by optimizing $\tilde{H}(x) = -a^*\|x - x_0\|_2^2$ along d starting from $x_0 + \delta_0 d$ at the N -th iteration, then x_N will be in an attraction basin of x' , if the basin ever exists.*

Theorem 3 can be explained intuitively as follows. Consider pushing a ball down the peak of a mountain with height $-f(x_1)$ (it can be regarded as the ball’s gravitational potential energy) along a direction d . The ball will keep moving until it arrives at a point $\tilde{x} = x_0 + \tilde{t}d$ for some \tilde{t} such that $f(x_1) = f(\tilde{x})$. For any $t \in [\delta_0, \tilde{t}]$, the ball has a positive velocity, i.e. $g(t) - g(t_1) > 0$ where $t_1 = \delta_0$. But the ball has a zero velocity at \tilde{t} , and negative at $t > \tilde{t}$. Hence $\int (f(x_0 + td) - f(x_1))dt$ reaches its maximum in $[0, \tilde{t}]$. The integral is approximated by its discrete sum, i.e. $F(a)$, in Alg. 2.

Further, according to the law of the conservation of energy, the ball will keep moving until at some \hat{t} , $f(x_0 + t\hat{d}) - f(x_1) = 0$ in which case $F'(a) = 0$. This means that the ball falls into the attraction basin of a smaller criterion than $f(x_1)$ as shown

in Fig. 4(b). Fig. 4(a) shows when a is small, in N iterations, the ball reaches some t_N but $F'(a) \approx \int_{t_1}^{t_N} (g'(t)) > 0$.

Moreover, if there is no smaller local minimizers in search region, the ball will keep going until it rolls outside the restricted search region bounded by M as shown in Fig. 4(e) which means Alg. 2 fails to find a^* . Fig. 4(c)(d) show the cases when there are more than one local minimizers within the search region.

Once such a^* has been found, the corresponding x_N will enter an attraction basin of a local minimum with smaller criterion than x_0 . If we cannot find such an a^* in the direction of d within a distance M to x_0 , we consider that there is no another smaller local minimum along d . If it is the case, d is non-promising. We thus set a negative score for it as shown in line 8 of Alg. 2.

It is seen that the running of line 5 of Alg. 2 requires to compute N gradients of $f(x)$ at each iteration. This causes Alg. 2 time consuming. We hereby propose to accelerate this procedure by fixing a but finding a proper number of iterations. Alg. 3 summarizes the fast policy. Given a direction d , during the search, the learning rate α and the escaping length controller a are fixed. At each iteration of Alg. 3, an iterate x_i is obtained by applying gradient descent over $\tilde{H}(x)$. The gradient of x_i over $f(x)$ is computed (line 6). $Q_i = \sum_{j=1}^i \nabla f(x_j)^\top (x_j - x_{j-1})$ is computed (line 7). Alg. 3 terminates if there is an i , such that $Q_i > 0$ and $Q_{i-1} < 0$ or the search is beyond the bound. It is seen that during the search, at each iteration, we only need to compute the gradient for once, which can significantly reduce the computational cost in comparison with Alg. 2.

Algorithm 3 Fast policy on finding a new starting point

Require: a local minimizer x_0 , a search direction d , a bound $M > 0$ and positive scalars a, δ_0, ϵ and α ;

Ensure: score u_d and x

- 1: set $i \leftarrow 1$ and $Q_i = 0$;
 - 2: compute $x_i \leftarrow x_{i-1} + \delta_0 d$ and $\nabla f(x_i)$;
 - 3: **repeat**
 - 4: set $s_Q \leftarrow Q_i$;
 - 5: $i \leftarrow i + 1$
 - 6: compute $x_i \leftarrow x_{i-1} - \alpha \cdot 2a(x_{i-1} - x_0)$ and $\nabla f(x_i)$;
 - 7: compute $Q_i \leftarrow Q_{i-1} + \nabla f(x_i)^\top (x_i - x_{i-1})$
 - 8: **until** $\{s_Q < 0 \ \& \ Q_i > 0\}$ or $\|x_i - x_0\| \geq M$
 - 9: compute $u_d = \max_{j=1, \dots, i} -\nabla f(x_j)^\top d$;
 - 10: if $\|x_N - x_0\| \geq M$, set $u_d \leftarrow -|u_d|$;
 - 11: **return** u_d and $x = x_i$.
-

Alg. 3 aims to find an integer i such that $Q_{i-1} < 0$ but $Q_i > 0$. The existence of such an i can be illustrated as follows. It is seen that $Q_i = aF'(a)$ (please see Eq. 31 in Appendix B). This implies that $Q_i = \int_{t_1}^{t_i} g'(t)dt$. When $\alpha \rightarrow 0$, we have i_1 and i_2 so that $|t_{i_1} - \xi| < \epsilon$ and $|t_{i_2} - T| < \epsilon$ for any $\epsilon > 0$, and $Q(i_1) < 0$ and $Q(i_2) > 0$. Thus, there exists an i such that $Q(i) > 0$ and $Q(i-1) < 0$.

Corollary 1 proves that if there exists a better local minimum x' along d , then applying Alg. 2 or Alg. 3, we are able to escape from the local attraction basin of x_0 .

3) *Policy on the sampling of promising directions:* In the following, we show how to sample directions that are of high probability to be promising. We first present a fixed policy, then propose to learn for an optimal policy by policy gradient.

Algorithm 4 Fixed policy on sampling promising direction

Require: a local minimizer x_0 , an integer $P > 0$ and $\sigma > 0$

Ensure: a set of candidate directions and starting points

- 1: sample N_0 directions $\{d_i\}_{i=1}^{N_0}$ uniformly at random; apply Alg. 2 or Alg. 3 to obtain their scores $\{u_i\}_{i=1}^{N_0}$ and $\{x_i\}_{i=1}^{N_0}$;
 - 2: set $\mathcal{S} \leftarrow \emptyset, \mathcal{D} \leftarrow \emptyset, t \leftarrow 1$.
 - 3: **repeat**
 - 4: sample
 - $\tilde{d} = \sum_{i: u_i < 0} u_i d_i - \sum_{i: u_i > 0} u_i d_i + \varepsilon, \varepsilon \sim \mathcal{N}(0, \sigma^2)$
 - 5: apply Alg. 2 or Alg. 3 to obtain \tilde{u} and \tilde{x} .
 - 6: **if** $\tilde{u} > 0$ **then**
 - 7: set $\mathcal{S} \leftarrow \mathcal{S} \cup \{\tilde{x}\}$ and $\mathcal{D} \leftarrow \mathcal{D} \cup \{\tilde{d}\}$.
 - 8: **end if**
 - 9: set $u_i \leftarrow u_{i+1}, 1 \leq i \leq N_0 - 1$ and $u_{N_0} \leftarrow \tilde{u}$;
 - 10: set $d_i \leftarrow d_{i+1}, 1 \leq i \leq N_0 - 1$ and $d_{N_0} \leftarrow \tilde{d}$;
 - 11: $t \leftarrow t + 1$.
 - 12: **until** $t \geq P$.
 - 13: **return** \mathcal{S} and \mathcal{D} .
-

Alg. 4 summarizes the fixed policy method. In Alg. 4, first a set of directions are sampled uniformly at random (line 1). Their scores are computed by Alg. 2 or Alg. 3. Archives used to store the directions and starting points are initialized (line 2). A direction is sampled by using a linear combination of previous directions with their respective scores as coefficients (line 4). If the sampled direction has a positive score, its score and the obtained starting point are included in the archive. The sets of scores and directions are updated accordingly in a FIFO manner (lines 9-10). The algorithm terminates if the number of sampling exceeds P .

We hope that the developed sampling algorithm is more efficient than that of the random sampling in terms of finding promising direction. P_r denotes the probability of finding a promising direction by using the random sampling, P_c be the probability by the fixed policy. Then in Appendix C, we will do some explanation why $P_c > P_r$.

4) *The transition:* In our MDP model, the probability transition $p(s_{t+1}|s_t, a_t)$ is deterministic. The determination of new starting point depends on the sampling of a new direction d_t and its score u_t . New state s_{t+1} is then updated in a FIFO manner. That is, at each time step, the first element $(\mathbf{u}_1, \mathbf{d}_1)$ in s_t is replaced by the newly sampled $(\mathbf{u}_t, \mathbf{d}_t)$.

All the proofs in this section are given in Appendix B.

C. Learning the Escaping Policy by Policy Gradient

In the presented policy, a linear combination of previous directions with their scores as coefficients is applied to sample a new direction. However, this policy is not necessarily optimal.

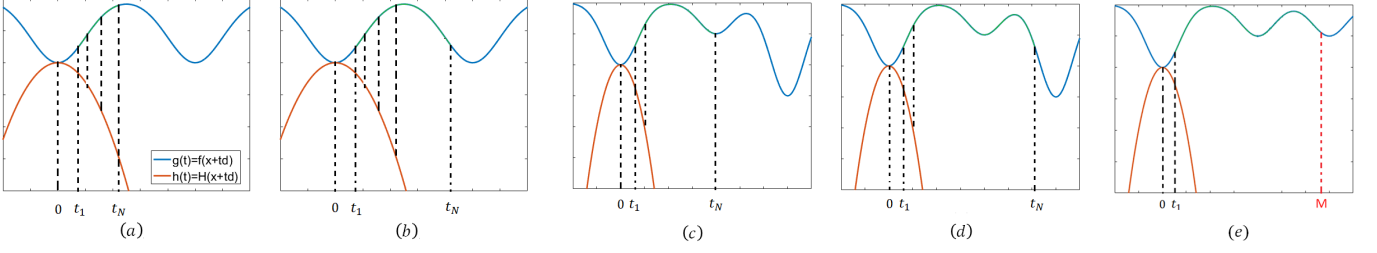


Fig. 4. Possible scenarios encountered when estimating a^* . (a) shows the case when a is not large enough, while (b) shows when a is appropriate. (c) shows that $x_N = x_0 + t_N d$ reaches a local minimum, but $F'(a) \neq 0$ because $g(t_N) - g(t_1) \neq 0$; (d) shows the case when there are more than one local minimizer. (e) shows when there is no smaller local minimizer within $\|x_N - x_0\| \geq M$.

In this section, we propose to learn an optimal policy by the policy gradient algorithm [35].

The learning is based on the same foregoing MDP framework. The goal is to learn the optimal coefficients for combining previously sampled directions. We assume that at time t , the coefficients are obtained as follows:

$$\begin{aligned} \mathbf{m}_t &= g(-|\mathbf{u}_t|; \theta); \\ \mathbf{w}_t &= -|\mathbf{u}_t| + \mathbf{m}_t; \end{aligned}$$

where $\mathbf{u}_t = [u_1, \dots, u_{N_0}]^\top$ and $\mathbf{d}_t = [d_1, \dots, d_{N_0}]$. $\mathbf{m}_t \in \mathbb{R}^{N_0}$ is the output of a feed-forward neural network g with parameter θ , and $\mathbf{w}_t \in \mathbb{R}^{N_0}$ is the coefficients. The current state s_t is the composition of \mathbf{u}_t and \mathbf{d}_t .

Fig. 5 shows the framework of estimating the coefficients and sampling a new direction at a certain time step. For the next time step, \mathbf{u}_{t+1} and \mathbf{d}_{t+1} are updated

$$\begin{aligned} u_i &= u_{i+1}, \text{ for } 1 \leq i \leq N_0 - 1 \text{ and } u_{N_0} = \tilde{u} \\ d_i &= d_{i+1}, \text{ for } 1 \leq i \leq N_0 - 1 \text{ and } d_{N_0} = \tilde{d} \end{aligned}$$

and $\mathbf{u}_{t+1} = \{u_i\}$, $\mathbf{d}_{t+1} = \{d_i\}$, $s_{t+1} = \{\mathbf{u}_{t+1}, \mathbf{d}_{t+1}\}$.

The policy gradient algorithm is used to learn θ for the neural network g . We assume that $\phi(s_t; \theta) = \mathbf{w}_t^\top \mathbf{d}_t$ and the policy can be stated as follows:

$$\pi(d|s_t) = \mathcal{N}(d|\phi(s_t; \theta), \sigma^2)$$

The reward is defined to be

$$\begin{aligned} r_1 &= \gamma \cdot \mathbb{I}(\tilde{u} > 0) \\ r_{t+1} &= \gamma^t \cdot \mathbb{I}(\tilde{u} > 0) \quad \text{if } r_{1:t-1} \text{ are all zero} \\ r_{t+1} &= 0 \quad \text{if } r_{1:t} \text{ are not all zero} \end{aligned} \quad (23)$$

where $\gamma = 0.9$ is a constant, \tilde{u} is the score of the sampled direction \tilde{d} and $\mathbb{I}(\cdot)$ is the indicator function.

Alg. 5 summarizes the policy gradient learning procedure for θ . θ is updated in E epochs. At each epoch, first a sample of trajectories is obtained (lines 3-23). Given x_0 , a trajectory can be sampled as follows. First, a set of N_0 initial directions is randomly generated and their scores are computed by Alg. 3 (lines 6-7). P new directions and their corresponding scores are then obtained (lines 9-22). At each step, the obtained direction \tilde{d} , the policy function $\phi(s_t; \theta)$ and the reward r_{t+1} are gathered in the current trajectory T_m (line 20). After the trajectory sampling, $\Delta\theta$ and θ_l are updated in lines 24- 28 and line 29, respectively.

Algorithm 5 Training policy network with policy gradient

Require: a local minimum x_0 , an integer $P > 0$, the number of training epochs E , the number of trajectories N_T , $\sigma > 0$ and learning rate $\beta > 0$.

Ensure: the optimal network parameter θ^* .

```

1: randomly initialize  $\theta_1 \in \mathbb{R}^d$ ;
2: for  $l = 1 : E$  do
3:   // create  $N_T$  trajectories
4:   for  $m = 1 : N_T$  do
5:     set  $T_m = \emptyset$ ;
6:     sample  $N_0$  directions  $\mathbf{d}_0 = \{d_i\}_{i=1}^{N_0}$  uniformly at random;
7:     apply Alg. 3 to obtain their scores  $\mathbf{u}_0 = \{u_i\}_{i=1}^{N_0}$  and  $\{x_i\}_{i=1}^{N_0}$ ;
8:     set  $\mathcal{S} \leftarrow \emptyset, \mathcal{D} \leftarrow \emptyset, t \leftarrow 0$ ;
9:     repeat
10:      // sample new direction
11:      sample  $\varepsilon \sim \mathcal{N}(0, \sigma^2)$ ;
12:      compute  $\phi(s_t; \theta) = \sum [-|u_i| + g(-|\mathbf{u}_t|; \theta)]_i d_i$  and  $\tilde{d} = \phi(s_t; \theta) + \varepsilon$ ;
13:      apply Alg. 3 to obtain  $\tilde{u}$ ;
14:      // update the state
15:      set  $r_{t+1}$  by Eq. 23
16:       $u_i = u_{i+1}, 1 \leq i \leq N_0 - 1$  and  $u_{N_0} = \tilde{u}$ ;
17:       $d_i = d_{i+1}, 1 \leq i \leq N_0 - 1$  and  $d_{N_0} = \tilde{d}$ ;
18:      set  $\mathbf{u}_{t+1} = \{u_i\}$ ,  $\mathbf{d}_{t+1} = \{d_i\}$  and  $s_{t+1} = \{\mathbf{u}_{t+1}, \mathbf{d}_{t+1}\}$ ;
19:      // update the trajectory
20:       $T_m \leftarrow T_m \cup \{\tilde{d}, \phi(s_t; \theta), r_{t+1}\}$ ;
21:       $t \leftarrow t + 1$ .
22:    until  $t \geq P$ .
23:  end for
24:  // policy gradient
25:   $\Delta\theta = 0$ 
26:  for  $m = 1 : N_T$  do
27:
28:  end for
29:   $\theta_{l+1} = \theta_l + \beta \Delta\theta$ ;
30: end for
31: return  $\theta^* \leftarrow \theta_{E+1}$ 

```

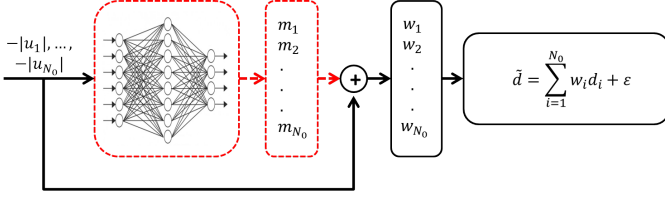


Fig. 5. The framework of the escaping policy on the t -th time step. The black solid line is the policy proposed in section IV-B. The red dash line covers the feed-forward network and its output.

D. Learning to be Global Optimizer

Combining the proposed local search algorithm and the escaping policy, we can form a global optimization algorithm. Alg. 6 summarizes the algorithm, named as L₂GO. Starting from an initial point x , Gd-Net is firstly applied to obtain a local minimizer (line 2). The escaping policy is applied to sample P new starting points (line 5). Gd-Net is then applied on these points (line 9). The algorithm terminates if the prefixed maximum number of escaping tries (i.e. K) has been reached (line 4), or no new promising directions can be sampled (line 6). If any of these conditions have been met, it is assumed that a global optimum has been found.

Algorithm 6 The proposed global optimization algorithm based on learning to learn (L₂GO).

Require: an initial point x , integers $K > 0$

Ensure: a global minimum x^*

```

1:  $k \leftarrow 1$ , stop = 0;
2: apply Gd-Net on  $x$  to obtain a local minimizer  $x_k$ ;
3: repeat
4:   if  $k \geq K$  stop = 1.
5:   apply the fixed escaping policy or the learned policy on
      $x_k$  to obtain a set  $\mathcal{S}$  containing new starting points.
6:   if  $\mathcal{S} = \emptyset$  then
7:      $x^* \leftarrow x_k$ , stop = 1.
8:   else
9:     apply Gd-Net to points in  $\mathcal{S}$  to obtain a set of local
       minimizers, denoted as  $\mathcal{S}^*$ .
10:    set  $x_k = \arg \min_{x \in \mathcal{S}^*} f(x)$ 
11:     $k \leftarrow k + 1$ .
12:   end if
13: until stop
14:  $x^* \leftarrow x_k$ 
15: return  $x^*$ .
```

Note. We should highlight that our method surpasses some filled function methods in the sense that our method has more chances to escape from local optimum. For example, consider the following filled function [37]:

$$H(x) = -a\|x - x_0\|^2 + \min\{0, f(x) - f(x_0)\}^3 \quad (24)$$

The existence of the stable point x_{fill} to H usually holds. But x_{fill} can be a saddle point or a local optimizer. If x_{fill} is a saddle point, then to escape x_0 , it is only possible by searching along $d_{\text{fill}} = x_{\text{fill}} - x_0$. However, it is highly unlikely d_{fill} be contained in the pre-fixed direction set of the traditional filled

function methods. This indicates that the corresponding filled function method will fail.

On the other hand, if x_{fill} is a local minimizer of $H(x)$, we can prove that the proposed policy can always find a promising solution. Theorem 4 summarizes the result.

Theorem 4. Suppose there exists an attraction basin of x_{fill} on the domain of $H(x)$, denoted as B_{fill} , then $\forall x \in B_{\text{fill}}$, we have $u_d > 0$ for $d = x - x_0$.

Proof. We first prove that $\forall x \in B_{\text{fill}}, d = x - x_0, \exists t \in \mathbb{R}$, s.t. $f(x_0 + t \cdot d) < f(x_0)$. This can be done by contradiction. If there is no such t , then

$$\nabla H(x_0 + t \cdot d) = -2at \cdot d. \quad (25)$$

This is because that $\forall t \in \mathbb{R}_{++}$, we have $f(x_0 + t \cdot d) \geq f(x_0)$, $H(x)$ degenerates to $-a\|t \cdot d\|^2$. Eq. 25 implies that apply gradient descent from x on $H(x)$ will not lead to a point in B_{fill} . This contradicts our assumption that $x \in B_{\text{fill}}$.

The existence of t implies $u_d > 0$ by Theorem 2. \square

V. EXPERIMENT RESULTS

In this section, we study the numerical performance of Gd-net, the escaping policies, and L₂GO.

A. Model-driven Local Search

This section investigates the performance of Gd-Net. In the experiments, 50 d-net blocks are used. Parameters of these blocks are the same.

Training. d-Net is trained through minimizing the Monte Carlo approximation to the loss functions as defined in Eq. 17, in which a sample of the Gaussian family \mathcal{F}_G is used. In the experiments, we use ten 2-d Gaussian functions with positive covariance matrix as the training functions. d-Net is trained on 25 initial points sampled uniformly at random for each training function. At each layer of d-Net, the step size α_k is obtained by exact line search in $[0, 1]$ ¹. Gradient descent is used to optimize Eq. 17 with a learning rate 0.1 for 100 epochs. The same training configuration is used in the following.

Testing. We use functions sampled from \mathcal{F}_G in 5-d, and χ^2 -functions² in 2-d to test Gd-Net. Note that Gd-Net is trained on 2-d \mathcal{F}_G . By testing on 5-d Gaussian functions, we can see its generalization ability on higher-dimensional functions. The testing on χ^2 functions can check the generalization ability of Gd-Net on functions with non-symmetric contour different to Gaussians. Fig. 6 shows the difference between Gaussian and χ^2 contour.

¹Note that taking $\alpha_k \in (0, 1]$ is not necessarily the best choice for line search. It is rather considered as a rule of thumb. Notice that limiting the search of α_k in $(0, 1]$ could make Gd-Net be scale-variant. We transform $f(x) = f(x)/f(x_0)$ in order to eliminate the scaling problem where x_0 is the initial point when testing.

²The χ^2 -function is of the following form

$$f(x) = \frac{x^{k/2-1}e^{-x/2}}{2^{k/2}\Gamma(k/2)}, x > 0$$

where $\Gamma(\cdot)$ is the gamma function and k is a parameter.

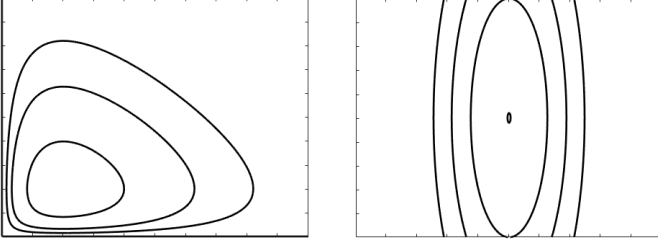


Fig. 6. A demo on the difference between a Gaussian contour and a χ^2 contour.

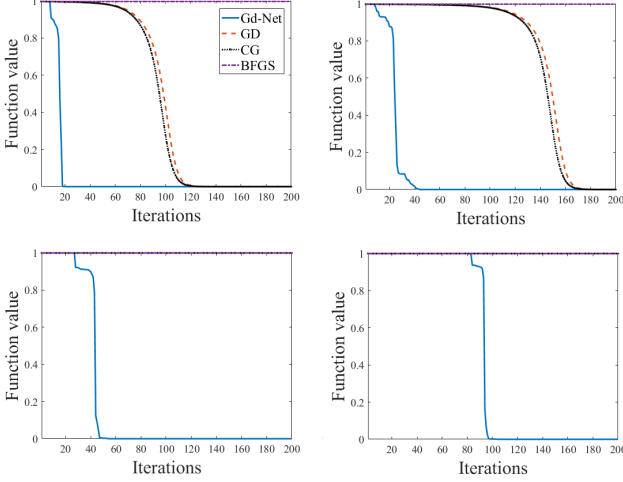


Fig. 7. The optimization curve of the learned Gd-Net on a 5-d Gaussian function with various initial points.

Fig. 7 shows the testing result of the learned Gd-Net on optimizing a 5-d Gaussian function with different initial points. The test on a χ^2 function is shown in Fig. 8. In these figures, first-order and second-order optimization algorithms, including steepest gradient descent, conjugate descent and BFGS, are used for comparison. From the figures, it is clear that Gd-Net requires much less iterations to reach the minimum than the compared algorithms.

Further, we observed that unlike BFGS, where a positive-definite Hessian matrix is a must, Gd-Net can cope with ill-conditioned Hessians. Fig. 9 shows the results on a 2-d Gaussian function with ill-posed Hessian. For an initial point that is far away from a minimizer, its Hessian is nearly singular which implies that the search area is rather flat. From the left plot of Fig. 9, it is seen that Gd-Net gradually decreases, while the other methods fail to make any progress. On the right plot, it is seen that Gd-Net finally progresses out the flat area and the criterion starts decreasing quickly.

B. The fixed escaping policy

In this section, controlled experiments are carried out to justify the ability of the fixed policy. We first consider a low-dimensional non-convex optimization problem with two local minimizers, then a high-dimensional highly non-convex problems with many local minimizers. The fixed policy is compared with random sampling on these test problems.

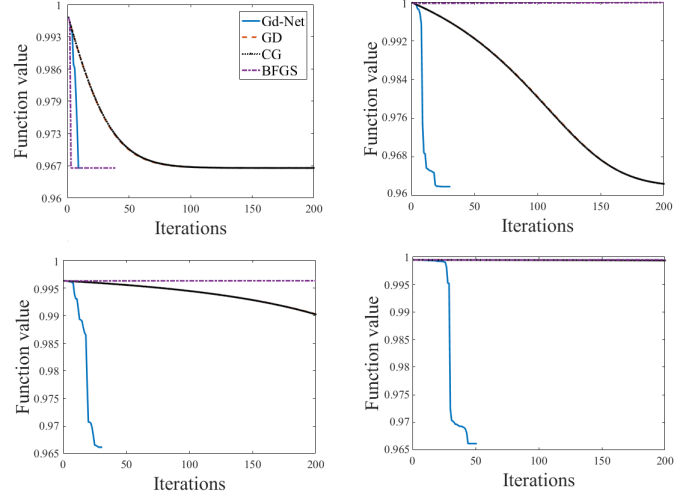


Fig. 8. The optimization curve of the learned Gd-Net on a 2-d χ^2 function with two different initial points.

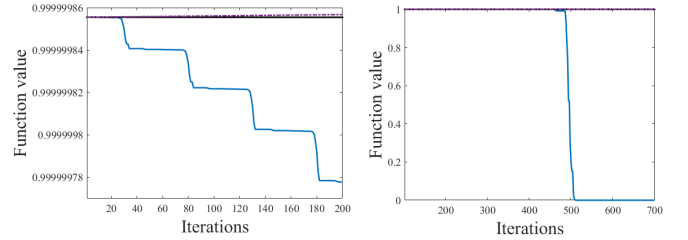


Fig. 9. The optimization procedure of Gd-Net (with 5 blocks) on a 5-d Gaussian function with an initial point far away from the optimum. The left plot shows the decreasing curve obtained by the first 4 blocks, while the right shows the curve of the rest block.

1) *Mixture of Gaussians functions*: Consider the following mixture of Gaussians functions

$$f(x) = -\sum_{i=1}^m c_i \exp \{-(x - \mu_i)^T \Sigma_i^{-1} (x - \mu_i)\} \quad (26)$$

where $x \in \mathbb{R}^n$, $c_i > 0$ and $\Sigma_i \succeq 0$. The mixture of Gaussian functions have m local minimizers at μ_i 's.

In the experiments, we set $m = 2, 3$. To test the ability of the escaping scheme, we assume the escaping starts from a local minimizer. We test on dimension $n = 2, 3, 5, 8, 10$. The other algorithmic parameters are $N_0 = 2, 3, 5, 8, 10$, $P = 15, 20, 50, 100, 250$ for $n = 2, 3, 5, 8, 10$, respectively, and $\sigma = 0.1$, $\delta_0 = 0.2$, $N = 20$.

Table I shows the average number of samplings used to escape from local optimum and the standard deviation (in brackets) over 500 runs obtained by using the fixed policy and the random sampling method.

From the table, it is observed that the fixed policy requires less samples than that of the random sampling, and the standard deviation is smaller. The p -value obtained by applying the rank sum hypothesis test at 5% significance level is shown in the last column. The hypothesis test suggests that the fixed policy outperforms the random sampling approach significantly (the p -value is less than 0.05).

TABLE I
THE NUMBER OF SAMPLINGS USED TO ESCAPE.

n	m	random search	fixed policy	p -value
2	2	4.25(3.51)	3.03(2.96)	0.00003
3	2	6.22(5.42)	4.75(4.55)	0.00003
5	2	12.38(13.07)	9.18(8.27)	0.00002
8	2	45.6(31.46)	39.5(30.12)	0.005
10	2	110.65(78.89)	99.6(74.78)	0.032
2	3	6.72(2.12)	5.53(0.96)	0.00003

2) *Deep neural network*: The loss function of a deep neural network has many local optimizers. We take the training of a deep neural network for image classification on CIFAR-10 as an example. For CIFAR-10, an 8-layer convolution neural network similar to Le-Net [38], with 2520-d parameters, is applied. The cross entropy is used as the loss function.

The number of local minimizers found by a method is used as the metric of comparison. Given a maximal number of attempts P , a larger number of local minimizers indicates a higher probability of escaping local minimum, and hence a better performance. For CIFAR-10, ADAM [17] with mini-batch stochastic gradient is applied in the minimization phase.

Note that existing filled functions often involve $f(x)$. This usually makes the application of mini-batch stochastic gradient method difficult if $f(x)$ is not sum of sub-functions. Instead, the auxiliary function $\tilde{H}(x)$ used in this paper does not involve $f(x)$. Fig. 10 shows the scores (cf. Eq. 21) against the distance to current local optimum with different mini-batch sizes. From the figure, it is seen that with different batch-size, the scores exhibit similar behavior. This shows the applicability of the proposed escaping method to stochastic-based local search algorithms. In the experiment, the parameters to apply Alg. 2 is set as $N_0 = 300$, $P = 1000$, $N = 10$, $\sigma = 0.01$, $a = 1$ and $\delta_0 = 0.5$.

In the following, the effective samplings³ in 1000 samplings are used to compare the proposed escaping policy against the random sampling. The obtained promising directions with different thresholds in 500 runs are summarized in Table II. It is clear that the proposed escaping policy is able to find more samples with positive scores than that of the random sampling.

TABLE II
THE NUMBER OF EFFECTIVE SAMPLINGS IN 1000 SAMPLINGS.

	score>0	score>0.01	score>0.03	score>0.05
random sampling	52	19	2	0
fixed policy	423	201	31	8

C. The fixed policy vs. the learned policy

In this section we show the effectiveness of the learned policy. The policy function $\phi(s_t; \theta)$ in Eq. 8 is set as a 3 layer network with sigmoid as hidden layer activation function, and a fully-connected output layer with linear activation function.

³A sampling is effective if the sampled direction is with positive score.

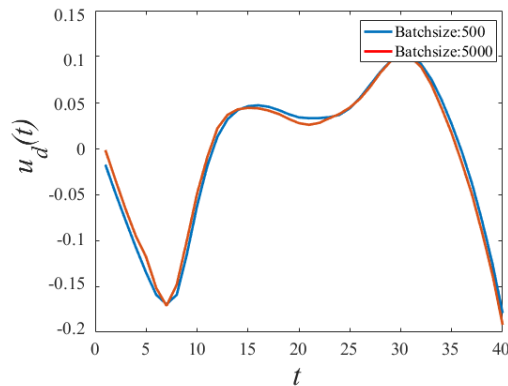


Fig. 10. The curves of the score against the step size w.r.t. two mini-batches when training a convolution neural network for CIFAR-10.

Training. A single Gaussian mixture function with two local minimizers is used for training the policy network in 2-d and 5-d, respectively. The other parameters are set $N_0 = 2(5)$; $P = 15(50)$; $N_T = 20(50)$ and $E = 30$ for 2 (5)-d. The number of hidden layer units is 5 and 200 for 2-d and 5-d, respectively.

Testing. To test the learned policy, we also use the Gaussian mixture functions with two local minimizers in 2-d and 5-d. Here we set $m = 2$, $c_1 = c_2 = 1$. Table III shows the average number of samplings used to escape from local optimum and the standard deviation (in brackets) over 500 runs obtained by using the fixed policy, the learned policy and the random sampling. Detailed configurations of the functions used for training can be found in Appendix D.

TABLE III
THE AVERAGE NUMBER OF SAMPLINGS USED TO FIND THE PROMISING DIRECTION IN DIFFERENT SETTINGS.

	n	random search	learned policy	fixed policy
1	2	4.25(3.51)	2.67(1.77)	3.03(2.96)
2	2	4.81(4)	3.07(2.05)	3.52(13.27)
3	2	7.03(5.45)	4.12(2.63)	5.5(4.87)
4	2	5.69(4.51)	3.37(2.23)	5.05(4.50)
5	5	12.76(10.77)	5.78(5.21)	10.22(9.35)
6	5	25.32(16.21)	13.08(11.96)	21.65(15.81)
7	5	16.16(13.15)	8.11(7.55)	11.68(10.61)
8	5	7.25(6.30)	4.01(4.32)	4.39(4.38)
9	5	11(10.29)	7.28(7.69)	8.48(7.95)

From the table, it is seen clearly that the learned policy requires less samplings to reach new local optimum. To observe the behaviors of the compared escaping policies better, Fig. 11 shows the histograms of the number of effective samplings for a 2-D function. From the figure, we see that the fixed policy is mostly likely to escape the current local optimum in one sampling, but it also is highly possible to require more samplings. That is, the number of effective samplings by the fixed policy follows a heavy-tail distribution. For the learned policy, the effective sampling numbers are mostly concentrated in the first 7 samplings. This shows that the learned policy is more robust than the other policies, which can also be confirmed in Table III by the standard deviations. We may

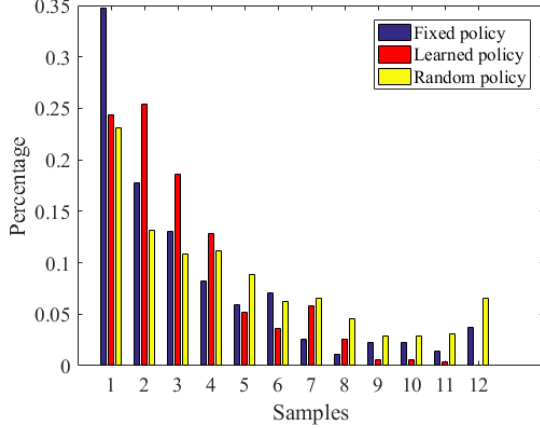


Fig. 11. The histogram of the number of effective samplings for a 2-D Gaussian mixture function by the fixed policy, the learned policy and the random sampling policy.

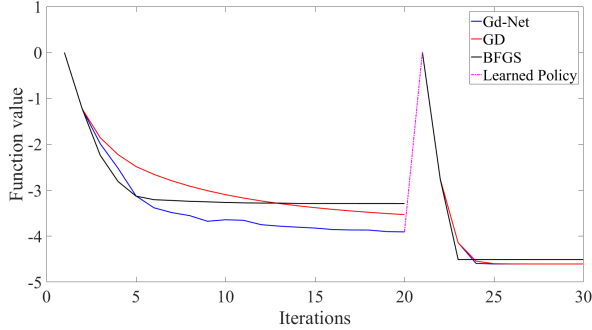


Fig. 12. The running procedure of L₂GO, in which GD, BFGS and Gd-Net are used as local search, while the learned policy is used to escape from local minimum (represented in pink dotted line).

thus conclude that the learned policy is more efficient than the fixed policy and random sampling.

D. The global search ability

In this section, we study the global search ability of L₂GO in comparison with the filled function method proposed in [8]. Three examples, including the three hump function, robust regression and neural network classifier, are used as benchmarks.

1) *Three-hump function*: The function is defined as

$$f(x) = 2x_1^2 - 1.05x_1^4 + x_1^6/6 - x_1x_2 + x_2^2.$$

It has three local minimizers at $[-1.73, -0.87]^\top$, $[0, 0]^\top$, and $[1.73, 0.87]^\top$. The global minimizer is at $[0, 0]^\top$. In our test, the algorithm parameters are set as $N_0 = 2$, $P = 15$, $\sigma = 0.1$, $\delta = 0.2$ and $N = 20$. We run L₂GO 20 times with different initial points. Fig. 12 shows the averaged optimization process of L₂GO. From the figure, it is seen that L₂GO is able to reach the local minimizer one by one. It is also seen that Gd-Net performs better than BFGS and steepest descent.

Table IV shows the number of effective samplings when using the fixed policy, random sampling and learned policy as escaping scheme. It is seen that the filled function method has failed due to the existence of the saddle point as shown in Fig. 3.

TABLE IV
THE NUMBER OF SAMPLINGS USED TO FIND THE PROMISING DIRECTIONS FOR THE THREE-HUMP FUNCTION.

random sampling	learned policy	fixed policy	filled function
5.35(4.38)	3.29(2.07)	3.76(3.26)	NA

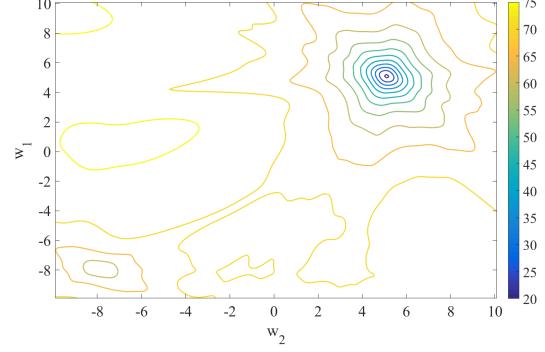


Fig. 13. The contour of the robust regression function with $w_1 = (-8, -8)$, $w_2 = (5, 5)$ and $b_1 = b_2 = 0$, respectively.

2) *Robust regression*: For the robust linear regression problem [20], a popular choice of the loss function is the Geman-McClure estimator, which can be written as follows:

$$\mathbf{P} : \min_{w, b} f(w, b) = \frac{1}{n} \sum_{i=1}^n \frac{(y_i - w^\top x_i - b)^2}{(y_i - w^\top x_i - b)^2 + c^2} \quad (27)$$

where $w \in \mathbb{R}^d$, $b \in \mathbb{R}$ represent the weights and biases, respectively. $x_i \in \mathbb{R}^d$ and $y_i \in \mathbb{R}$ is the feature vector and label of the i -th instance and $c \in \mathbb{R}$ is a constant that modulates the shape of the loss function.

The landscape of the robust regression problem can be systematically controlled. Specifically, we can decide the number of local minimizers, their locations and criteria readily. Note that given $\{w, b\}$, the training data can be created by

$$y_i = w^\top x_i + b_i + \epsilon \quad (28)$$

Different $\{w, b\}$ indicates different local minimum.

In our experiments, we randomly sample 50 points of $x_j \sim \mathcal{N}(0, \mathbb{I})$ in \mathbb{R}^2 , and divide them to two sets $\mathcal{S}_1 = \{x_j, 1 \leq i \leq 10\}$ and $\mathcal{S}_2 = \{x_j, 11 \leq i \leq 50\}$. For each set \mathcal{S}_i , $1 \leq i \leq 2$, give a $\{w_i, b_i\}$, apply $y_j = w_i^\top x_j + b_i + \epsilon$, a training set \mathcal{T}_i can be obtained. Combining them, we obtain the whole data set $\mathcal{T} = \cup \mathcal{T}_i$. Given this training set, it is known that the objective function has two obvious local minimizers at (w_1, b_1) and (w_2, b_2) and lots of other local minimizers. Please see Fig. 13 for contour of the robust regression function with $w_1 = (-8, -8)$, $w_2 = (5, 5)$ and $b_1 = b_2 = 0$. There are two main local minimizers at (w_1, b_1) and (w_2, b_2) with $f(w_2, b_2) < f(w_1, b_1)$, and many other local minimizers.

Fig. 14 shows the optimization curve of the robust regression function, in which Gd-Net and GD are compared. We notice that BFGS is not convergent in this case since landscape here is very flat. From the figure, we can see that for robust regression function, Gd-Net also performs better than GD. Table V shows the average numbers of effective samplings

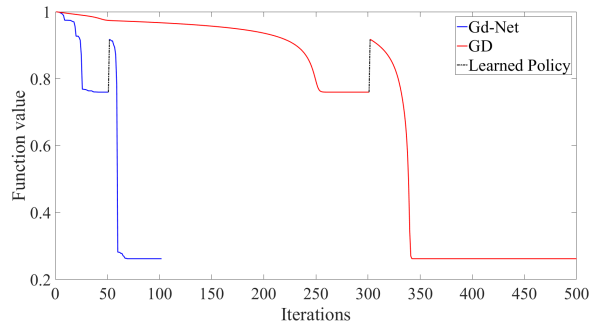


Fig. 14. The optimization procedure of L_2GO and the steepest gradient with the learned policy on robust regression.

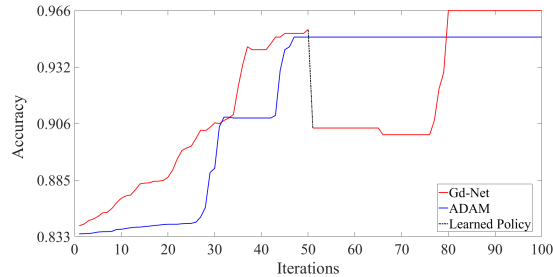


Fig. 15. The optimization curve of L_2GO and ADAM on training the classification network.

obtained by the compared policies. From the table it is clear that the learned policy performs the best, while the filled function method needs much more times.

TABLE V

THE NUMBER OF SAMPLINGS USED TO FIND THE PROMISING DIRECTIONS FOR ROBUST REGRESSION FUNCTION.

random sampling	fixed policy	learned policy	filled function
13.05(9.48)	11.3(8.83)	12.23(9.27)	89(20.22)

3) *neural network classifier*: We construct a small network with one hidden layer for a classification problem in 2-d [20]. The number of hidden layer is one, and the total dimension of network is 5. The goal is to classify $\mathcal{S}_i = \{x_i + \varepsilon | \varepsilon \sim \mathcal{N}(0, \sigma^2)\}, i = 1, 2$ into two classes, where $x_1 \neq x_2 \in \mathbb{R}^2$. The cross entropy is used as the loss function. ADAM is compared with L_2GO . In ADAM, the learning rate is 0.001, and the hyper-parameters for momentum estimation are 0.9 and 0.9.

Fig. 15 shows the optimization curve. From the figure, we see that L_2GO performs better than ADAM. It can escape from the local optimum, and reach a better optimum successfully.

VI. CONCLUSION AND FUTURE WORK

This paper proposed a two-phase global optimization algorithm for smooth non-convex function. In the minimization phase, a local optimization algorithm, called Gd-Net, was obtained by the model-driven learning approach. The method was established by learning the parameters of a non-linear combination of different descent directions through deep neural network training on a class of Gaussian family function. In

the escaping phase, a fixed escaping policy was first developed based on the modeling of the escaping phase as an MDP. We further proposed to learn the escaping policy by policy gradient.

A series of experiments have been carried out. First, controlled experimental results showed that Gd-Net performs better than classical algorithms such as steepest gradient descent, conjugate descent and BFGS on locally convex functions. The generalization ability of the learned algorithm was also verified on higher dimensional functions and on functions with contour different to the Gaussian family function. Second, experimental results showed that the fixed policy was more able to find promising solutions than random sampling, while the learned policy performed better than the fixed policy. Third, the proposed two-phase global algorithm, L_2GO , showed its effectiveness on a benchmark function and two machine learning problems.

In the future, we plan to work on the following avenues. First, since the Hessian matrix is used in Gd-Net, it is thus not readily applicable to high-dimensional functions. Research on learning to learn approach for high-dimensional functions is appealing. Second, we found that learning the escaping policy is particularly difficult for high-dimensional functions. It is thus necessary to develop a better learning approach. Third, the two-phase approach is not the only way for global optimization. We intend to develop learning to learn approaches based on other global methods, such as branch and bound [39], and for other types of optimization problems such as non-smooth, non-convex and non-derivative.

REFERENCES

- [1] L. Dixon and G. Szegő, *Towards Global Optimization*. New York: Elsevier, 1975.
- [2] R. Horst and P. Pardalos, Eds., *Handbook of Global Optimization*. Dordrecht: Kluwer, 1995.
- [3] (2019). [Online]. Available: <https://www.mat.univie.ac.at/~neum/glopt.html>
- [4] J. Pinter, "Continuous global optimization: Applications," in *Encyclopedia of Optimization*, C. Floudas and P. Pardalos, Eds. Boston, MA.: Springer, 2008.
- [5] A. Neumaier, "Convexification and global optimization in continuous global optimization and constraint satisfaction," in *Acta Numerica*, A. Iserles, Ed. Cambridge University press, 2004.
- [6] P. Gary, W. Hart, L. Painton, C. Phillips, M. Trahan, and J. Wagner, "A survey of global optimization methods," 1997.
- [7] A. Levy and S. Gómez, "The tunneling method applied to global optimization," in *Numerical Optimization*, P. Boggs, R. Byrd, and R. Schnabel, Eds. SIAM, 1985.
- [8] R. P. Ge and Y. F. Qin, "A class of filled functions for finding global minimizers of a function of several variables," *Journal of Optimization Theory and Applications*, vol. 54, no. 2, pp. 241–252, 1987.
- [9] S. Boyd and L. Vandenberghe, *Convex optimization*. Cambridge university press, 2004.
- [10] R. Fletcher and C. M. Reeves, "Function minimization by conjugate gradients," *Computer Journal*, vol. 7, no. 2, pp. 149–154, 1964.
- [11] D. H. Wolpert and W. G. Macready, "No free lunch theorems for optimization," *IEEE Transactions on Evolutionary Computation*, vol. 1, no. 1, pp. 67–82, 1997.
- [12] W. Sun and Y. Yuan, *Optimization theory and methods: nonlinear programming*. Springer Science & Business Media, 2006, vol. 1.
- [13] D. W. Marquardt, "An algorithm for least-squares estimation of non-linear parameters," *Journal of the society for Industrial and Applied Mathematics*, vol. 11, no. 2, pp. 431–441, 1963.
- [14] B. T. Polyak, "Some methods of speeding up the convergence of iteration methods," *USSR Computational Mathematics and Mathematical Physics*, vol. 4, no. 5, pp. 1–17, 1964.

- [15] J. Duchi, E. Hazan, and Y. Singer, "Adaptive subgradient methods for online learning and stochastic optimization," *Journal of Machine Learning Research*, vol. 12, no. Jul, pp. 2121–2159, 2011.
- [16] M. D. Zeiler, "Adadelta: an adaptive learning rate method," *arXiv preprint arXiv:1212.5701*, 2012.
- [17] D. P. Kingma and J. Ba, "Adam: A method for stochastic optimization," in *ICLR*, 2015.
- [18] M. Andrychowicz, M. Denil, S. Gomez, M. W. Hoffman, D. Pfau, T. Schaul, B. Shillingford, and N. De Freitas, "Learning to learn by gradient descent by gradient descent," in *NIPS*, 2016, pp. 3981–3989.
- [19] S. Hochreiter and J. Schmidhuber, "Long short-term memory," *Neural Computation*, vol. 9, no. 8, pp. 1735–1780, 1997.
- [20] K. Li and J. Malik, "Learning to optimize," in *ICLR*, 2017.
- [21] Y. Chen, Hoffman, M. W. S. G. Colmenarejo, M. Denil, T. P. Lillicrap, and N. de Freitas, "Learning to learn without gradient descent by gradient descent," *ICML*, 2017.
- [22] Z. Xu and J. Sun, "Model-driven deep-learning," *National Science Review*, vol. v.5, no. 1, pp. 26–28, 2018.
- [23] J. Sun, H. Li, Z. Xu *et al.*, "Deep admm-net for compressive sensing mri," in *NIPS*, 2016, pp. 10–18.
- [24] S. Wang, J. Sun, and Z. Xu, "Hyperadam: A learnable task-adaptive adam for network training," in *AAAI*, 2019.
- [25] K. Lv, S. Jiang, and J. Li, "Learning gradient descent: Better generalization and longer horizons," in *ICML*, 2017, pp. 2247–2255.
- [26] A. Levy and A. Montalvo, "The tunneling algorithm for the global minimization of functions," *SIAM Journal on Scientific and Statistical Computing*, 1985.
- [27] Y. Xu, Y. Zhang, and S. Wang, "A modified tunneling function method for non-smooth global optimization and its application in artificial neural network," *Applied Mathematical Modelling*, vol. 39, pp. 6348–6450, 2015.
- [28] H. Lin, Y. Wang, and L. Fan, "A filled function method with one parameter for unconstrained global optimization," *Applied Mathematical Modelling*, vol. 218, pp. 3776–3785, 2011.
- [29] Y. Zhang, L. Zhang, and Y. Xu, "New filled functions for non-smooth global optimization," *Applied Mathematical Modelling*, vol. 33, no. 7, pp. 3114–3129, 2009.
- [30] L. Zhang, C. Ng, D. Li, and W. Tian, "A new filled function method for global optimization," *Journal of Global optimization*, vol. 28, no. 1, pp. 17–43, 2004.
- [31] S. Ma, Y. Yang, and H. Liu, "A parameter-free filled function for unconstrained global optimization," *Applied Mathematics and Computation*, vol. 215, no. 10, pp. 3610–3619, 2010.
- [32] K. Arulkumaran, M. P. Deisenroth, M. Brundage, and A. A. Bharath, "Deep reinforcement learning: A brief survey," *IEEE Signal Processing Magazine*, vol. 34, no. 6, pp. 26–38, 2017.
- [33] D. Silver, A. Huang, C. J. Maddison, A. Guez, L. Sifre, G. Van Den Driessche, J. Schrittwieser, I. Antonoglou, V. Panneershelvam, M. Lanctot *et al.*, "Mastering the game of go with deep neural networks and tree search," *Nature*, vol. 529, no. 7587, p. 484, 2016.
- [34] V. Mnih, K. Kavukcuoglu, D. Silver, A. Graves, I. Antonoglou, D. Wierstra, and M. Riedmiller, "Playing atari with deep reinforcement learning," *arXiv preprint arXiv:1312.5602*, 2013.
- [35] R. Sutton and A. Barto, *Reinforcement Learning: An Introduction*, 1998.
- [36] R. Wilson, "Multiresolution gaussian mixture models: Theory and applications," in *IEEE International Conference on Pattern Recognition*. Citeseer, 2000.
- [37] Y. Liang, L. Zhang, M. Li, and B. Han, "A filled function method for global optimization," *Journal of Computational and Applied Mathematics*, vol. 205, no. 1, pp. 16–31, 2007.
- [38] Y. LeCun, L. Bottou, Y. Bengio, P. Haffner *et al.*, "Gradient-based learning applied to document recognition," *Proceedings of the IEEE*, vol. 86, no. 11, pp. 2278–2324, 1998.
- [39] E. L. Lawler and D. E. Wood, "Branch-and-bound methods: A survey," *Operations Research*, vol. 14, no. 4, pp. 699–719, 1966.

APPENDIX A

The proof of Theorem 1 can be found below.

Proof. In the AGD, $d_k = -R_{k-1}\tilde{H}_{k-1}g_k$ where

$$R_{k-1} = I - \frac{s_{k-1}\hat{y}_{k-1}^\top}{s_{k-1}^\top\tilde{y}_{k-1}},$$

$\tilde{y}_{k-1} = w_k^3g_k - w_k^4g_{k-1}$, $\hat{y}_{k-1} = w_k^1g_k - w_k^2g_{k-1}$, and $\tilde{H}_{k-1} = \beta_k H_{k-1} + (1 - \beta_k)I$. With exact linear search, we have $g_k^\top s_{k-1} = 0$, therefore

$$\begin{aligned} -g_k^\top d_k &= g_k^\top (\beta_k H_{k-1} + (1 - \beta_k)I)g_k \\ &\quad - g_k^\top \frac{s_{k-1}\hat{y}_{k-1}^\top}{s_{k-1}^\top\tilde{y}_{k-1}}\tilde{H}_{k-1}g_k \\ &= g_k^\top (\beta_k H_{k-1} + (1 - \beta_k)I)g_k \end{aligned}$$

It is clear that $-g_k^\top d_k > 0$ if $H_{k-1} \succ 0$, otherwise a $\beta_k > 0$ can be chosen to make $(\beta_k H_{k-1} + (1 - \beta_k)I)$ diagonally dominant, which means $g_k^\top (\beta_k H_{k-1} + (1 - \beta_k)I)g_k > 0$. Therefore, we can always make sure $g_k^\top d_k < 0$, i.e. d_k is a descent direction, and

$$f(x_1) \geq f(x_2) \geq \dots \geq f(x_k)$$

Since $f(x)$ is bounded, there exists $f(x^*)$ such that $\lim_{k \rightarrow \infty} f(x_k) = f(x^*)$. \square

APPENDIX B

This section gives details of the proofs for the theorems in Section III. The proof to Theorem 2 is shown below.

Proof. According to assumption (2), $g(t)$ is convex in $[-\delta, \delta]$. As $g'(0) = f'(x)|_{x=x_0} = 0$, $g''(0) > 0$, then $g'(t) > 0$ in $(0, \delta]$. Therefore, $g(t)$ is monotonically increasing in $[0, \delta]$, and monotonically decreasing in $[T - \delta, T]$. Since $f(x) \in C^2(\mathbb{R}^n)$, then $g(t) \in C^2[0, T]$. This implies that $g'(t)$ is continuous in $[0, T]$.

Since $g'(\delta) > 0$ and $g'(T - \delta) < 0$, then there exists a ξ such that $g'(\xi) = 0$. Further, ξ is unique since it is assumed that there is no other local minima between x_0 and x_1 . Then we have $g'(t) > 0$ in $[0, \xi)$, and $g'(t) < 0$ in $(\xi, T]$. \square

To prove Theorem 3, we first prove Lemma 5.

Lemma 5. Suppose $F(a)$ to be the function defined in Alg. 2. For fixed a and N , we have:

$$\lim_{\alpha \rightarrow 0} F'(a) = \frac{1}{a} \int_{t_1}^{t_N} g'(t)dt \quad (29)$$

where $g(t) = f(x_0 + td)$.

Proof. Since $\{x_1, \dots, x_N\}$ are all on the line $x_0 + td$ with $t > 0$. Therefore, each x_i , $1 \leq i \leq N$ can be written as

$$x_i = x_0 + t_i d$$

where $t_1 = \delta_0 > 0$ and $t_1 < t_2 < \dots < t_N$. Further, we have

$$x_i - x_{i-1} = 2a\alpha t_{i-1}d \Leftrightarrow (t_i - t_{i-1}) \cdot d = 2a\alpha t_{i-1}d$$

or equivalently,

$$t_i - t_{i-1} = 2a\alpha t_{i-1} \implies t_i = (1 + 2a\alpha)^{i-1}t_1 \quad (30)$$

We thus have:

$$\begin{aligned}
F'(a) &= \sum_{i=1}^N \nabla_a f(x_i)/(i-1) \\
&= \sum_{i=2}^N \nabla_a f((1+2a\alpha)^{i-1}t_1d)/(i-1) \\
&= \sum_{i=2}^N \nabla f((1+2a\alpha)^{i-1}t_1d)^\top \cdot 2\alpha t_{i-1}d \\
&= \sum_{i=2}^N \nabla f(x_{i-1} + a \cdot 2\alpha t_{i-1}d)^\top \cdot \frac{1}{a}(t_i - t_{i-1})d \\
&= \frac{1}{a} \sum_{i=2}^N \nabla f(x_i)^\top \cdot d \cdot (t_i - t_{i-1}) \\
&= \frac{1}{a} \sum_{i=2}^N g'(t_i)(t_i - t_{i-1})
\end{aligned} \tag{31}$$

Since $g'(t)$ is continuous in $[t_1, t_N]$, it is Riemann integrable. Thus, for a fixed N , we have

$$\lim_{\alpha \rightarrow 0} \sum_{i=2}^N g'(t_i)(t_i - t_{i-1}) = \int_{t_1}^{t_N} g'(t)dt$$

This finishes the proof. \square

In the sequel, we define

$$G(a) = t_N - t_1 = ((1+2\alpha a)^{N-1} - 1)t_1$$

where $a \in [0, \infty)$. Here $G(a)$ is just the distance between x_N and x_1 along d . Obviously, $G(a)$ is a polynomial function of a , and it is monotonically increasing.

Based on Lemma 5, Lemma 6 can be established.

Lemma 6. Suppose that $x' = x_0 + Td$ is a point such that $f(x_0) \geq f(x')$, and there are no other local minimizer within \mathcal{B}_0 . If α is sufficiently small, then there exists an a^* such that $F'(a^*) = 0$.

Proof. Since $f(x') \leq f(x_0)$, and $g(t) = f(x_0 + td)$ is smooth, there exists a ξ such that $\xi = \arg \max_{t \in [t_1, T]} g(t)$.

Let's consider two cases. First, let $D_1 = \xi - t_1$, then there is an a_1 s.t. $G(a_1) = D_1$ according to the intermediate value theorem. As α is sufficiently small, we have: $\forall \varepsilon > 0, \exists \alpha$ s.t.

$$\left| F'(a_1) - \frac{1}{a_1} \int_{t_1}^{t_N} g'(t)dt \right| < \varepsilon$$

Note that we can choose δ_0 s.t.

$$\begin{aligned}
\frac{1}{a_1} \int_{t_1}^{t_N} g'(t)dt &= \frac{1}{a_1} (g(\xi) - g(t_1)) = \\
&\frac{1}{a_1} (f(x_0 + \xi d) - f(x_0 + \delta_0 d)) > 0
\end{aligned}$$

Let $\epsilon_0 = \frac{1}{a_1} \int_{t_1}^{t_N} g'(t)dt$ and $\epsilon = \epsilon_0/2$, then $\exists \alpha_0$ s.t. $|F'(a_1) - \epsilon_0| < \epsilon_0/2 \Rightarrow F'(a_1) > \epsilon_0/2 > 0$.

Similarly, if let $D_2 = T - t_1$, then there is a_2 s.t. $G(a_2) = D_2$, as α is sufficiently small, we have: $\forall \varepsilon > 0, \exists \alpha$ s.t.

$$\left| F'(a_2) - \frac{1}{a_2} \int_{t_1}^{t_N} g'(t)dt \right| < \varepsilon$$

Note that

$$\begin{aligned}
\frac{1}{a_2} \int_{t_1}^{t_N} g'(t)dt &= \frac{1}{a_2} (g(T) - g(t_1)) = \\
\frac{1}{a_2} [f(x') - f(x_0 + \delta_0 d)] &= \frac{1}{a_2} (f(x') - f(x_1)) < 0
\end{aligned}$$

Let $\epsilon_1 = \frac{1}{a_2} \int_{t_1}^{t_N} g'(t)dt$ and $\epsilon = -\epsilon_1/2$, then $\exists \alpha_0$ s.t. $|F'(a_2) - \epsilon_1| < -\epsilon_1/2 \Rightarrow F'(a_2) < \epsilon_1/2 < 0$.

In summary, we have $F'(a_1) > 0$ and $F'(a_2) < 0$, according to the intermediate value theorem, there exists an a^* such that $F'(a^*) = 0$. \square

If there are L local minimizers x^1, \dots, x^L in \mathcal{B}_0 whose criteria are bigger than $f(x_0)$, and a local minimizer x' with smaller criterion outside \mathcal{B}_0 . Denote $f_{\min} = \min_{i=1, \dots, L} \{f(x^i)\}$, we have $L+1$ local maximizers $\xi_1 < \dots < \xi_{L+1}$. Since $f(x') < f(x_0)$, we can set δ_0 such that $f_{\min} > f(x_0 + \delta_0 d)$. Substituting ξ_{L+1} to ξ in the proof, we can prove Theorem 3.

APPENDIX C

In the following, we will explain why $P_c > P_r$. In Alg. 4, the main idea is using negative linear combination and adding a noise to make algorithm robustly. Now we will explain the insight of 'negative linear combination'. We first assume that there are two local minimizers. Without loss of generality, suppose that we are at a local minimum x_0 , and there exists a local minima x' ($f(x') < f(x_0)$). Then x' has a neighborhood region $R_{x'}$, which satisfies $f(x) < f(x_0), \forall x \in R_{x'}$, then x'' denotes the center of circumscribed sphere of $R_{x'}$. Then $d^* \triangleq x'' - x_0$ is called the central direction in the sequel. Further, we define the ray $\ell_d = x_0 + td, t > 0$. We have the following Lemma 7.

Lemma 7. Given an initial sample of directions and scores $\{(d_1, u_1) \dots, (d_{N_0}, u_{N_0})\}$ ($N_0 \leq n$), using negative linear combination of d_1, \dots, d_{N_0} , it is of higher probability to obtain d^* than that of the random sampling.

Proof. In the following, we first prove the theorem in case $n = 2$. It is then generalized to $n > 2$.

In case $N_0 = 2$ and $n = 2$, suppose at some time step, we have two linearly independent directions d_1 and d_2 with negative scores. Let $\Omega = \{x : \|x - x_0\|_2 \leq M\}$ be the confined search space. The search space can then be divided into four regions B^1, B^2, B^3 and B^{*4} . Particularly, $B^* = \{d = \alpha_1 d_1 + \alpha_2 d_2, \alpha_1 < 0, \alpha_2 < 0\}$. Suppose that x' has a neighborhood region $R_{x'}$, which satisfies $f(x) < f(x_0), \forall x \in R_{x'}$, and the radius of the circumscribed sphere of $R_{x'}$ is r_0 . The boundary of the circumscribed sphere and x_0 can form a cone C^* . By assumption, the lines $\ell_{d_i}, i = 1, 2$ has no interaction with C^* (otherwise we have found a direction that will lead to the attraction basin of x'), i.e.

$$C^* \cap \{x | x \in \ell_{d_i}\} = \emptyset, \forall i \in \{1, 2\}$$

⁴Namely, $B^1 = \{d = \alpha_1 d_1 + \alpha_2 d_2, \alpha_1 > 0, \alpha_2 < 0\}$, $B^2 = \{d = \alpha_1 d_1 + \alpha_2 d_2, \alpha_1 < 0, \alpha_2 > 0\}$, $B^3 = \{d = \alpha_1 d_1 + \alpha_2 d_2, \alpha_1 > 0, \alpha_2 > 0\}$.

For each d_i , take x^i and x^* such that $x^i = \partial\Omega \cap \ell_{d_i}$ and $x^* = \partial\Omega \cap \ell_{d^*}$, respectively. Then the boundary of $B(x^i, r_1)$ and x_0 form a cone C^i , where

$$r_1 = \max_r \{B(x^*, r) \subset C^*\} \quad (32)$$

Let $\tilde{C} = \bigcup_{i=1}^2 C^i$, we have

$$\tilde{C} \cap \{x|x \in \ell_{d^*}\} = \emptyset$$

Thus, we should avoid looking for directions in the union of C^i 's.

Notice that if $B^* \cap C^i = \emptyset$ for $i = 1, 2$. Denote $\tilde{\Omega} = \{x|x \in \Omega, x \notin \tilde{C}\}$, then \tilde{P}_c , the probability of finding d^* in Ω by the negative linear combination, can be computed as follows:

$$\begin{aligned} \tilde{P}_c &= P\{\tilde{d} = d^*; x'' \in B^*\} + P\{\tilde{d} = d^*; x'' \notin B^*\} \\ &= P\{x'' \in B^*\} P\{\tilde{d} = d^* | x'' \in B^*\} \end{aligned}$$

where \tilde{d} is the direction got by negative linear combination. Notice that $P\{\tilde{d} = d^* | x'' \in B^*\} = \frac{V_{d^*}}{V_{B^*}}$ where V_{d^*}, V_{B^*} is the measure of d^*, B^* , respectively. Denote \tilde{P}_r the probability of finding d^* in Ω by random sampling, then V_{d^*} can be represented by \tilde{P}_r and the measure of Ω . That is, $V_{d^*} = \tilde{P}_r \cdot V_\Omega$. As d^* does not interact with \tilde{C} , thus $x'' \notin \tilde{C}$. Then we have:

$$\tilde{P}_c = \frac{V_{B^*}}{V_\Omega} \cdot \frac{\tilde{P}_r \cdot V_\Omega}{V_{B^*}} = \frac{V_\Omega}{V_\Omega} \cdot \tilde{P}_r > \tilde{P}_r$$

where $V_\Omega, V_{\tilde{\Omega}}$ is the measure of Ω and $\tilde{\Omega}$, respectively. The last inequality holds because $\tilde{\Omega} \subset \Omega$.

If $B^* \cap C^i \neq \emptyset$ for $i = 1, 2$, then B^i is covered by C^i . Since the region covered by C^i ($i = 1, 2$) in B^3 has a larger measure than B^* , B^* is thus the best region for sampling.

In case $n > 2$, we have n directions with negative scores d_1, \dots, d_n . If set d_2 as the subspace $S = \{d = \sum_{i=2}^n \alpha_i d_i, \alpha_i > 0\}$, since S has a zero measure in \mathbb{R}^n , the proof degenerates into the $n = 2$ case. \square

Furthermore, we will present why $P_c > P_r$:

We illustrate by using C^2 in Fig. 16 in $n = 2$. In Fig. 16, d_2 is a direction with negative score. If we want to create \tilde{d} which is a promising direction, then d^* must be between d_{low} and d_{up} as shown in Fig. 17.

To define d_{low} and d_{up} , let C_d is the cone made by the boundary of $B(x_d, r_1)$ and x_0 where $x_d = \partial\Omega \cap \ell_d$ for any $t > 0$ and d , and r_1 is defined in Eq. 32. We further define $D_{\tilde{d}} = \{d|\tilde{d} \in C_d \text{ and } C_d \cap \ell_{d_2} = \emptyset\}$ and $R = \{d|d \in D_{\tilde{d}}\}$. d_{low} and d_{up} are considered as the ray from x_0 to the boundary of R . Similarly to the definition of x_d , we define $x_{\tilde{d}} = \partial\Omega \cap \ell_{\tilde{d}}$, $x_{d_{\text{up}}} = \partial\Omega \cap \ell_{d_{\text{up}}}$ and $x_{d_{\text{low}}} = \partial\Omega \cap \ell_{d_{\text{low}}}$.

If the distance between x^2 and $x_{\tilde{d}}$ is larger, then the distance between $x_{d_{\text{up}}}$ and $x_{d_{\text{low}}}$ must be larger as shown in Fig. 17. This implies the probability that \tilde{d} is promising is higher. When the distance between x^2 and $x_{\tilde{d}}$ is larger than r_1 , i.e. $\tilde{d} \notin C^2$, the probability is the maximum since there is no d such that $C_d \cap \ell_{d_2} \neq \emptyset$ and $\tilde{d} \in C_d$. Therefore, it is the best to use the opposite direction of d_2 since the point by interacting $-d_2$ and Ω is the furthest to x_2 .

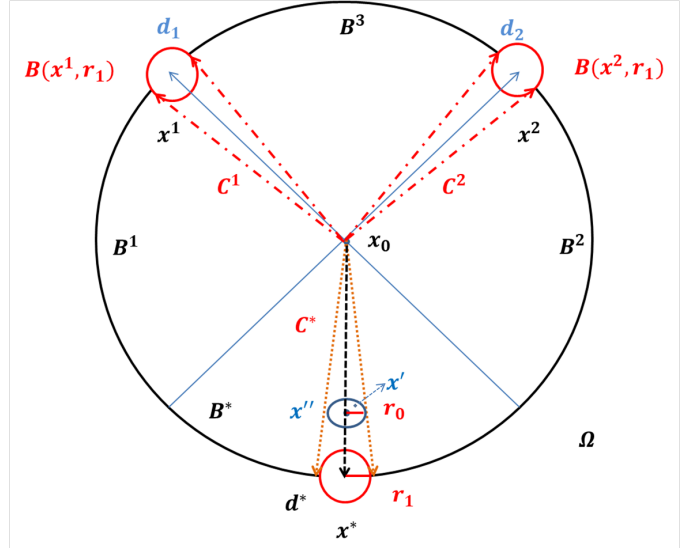


Fig. 16. Illustration of Lemma 7 in 2-D case. In the figure, d^* is to be found in Ω . r_0 is the radius of the circumscribed sphere of the attraction basin of x' . $x_0, B(x', r_0)$ form a cone C^* . For each d_i , take $x^i \in \partial\Omega \cap \ell_{d_i}$, the boundary of $B(x^i, r_1)$ and x_0 forms a cone C^i . Then $C^i \cap \{x|x = x_0 + td^*, x \in \Omega, t > 0\} = \emptyset, \forall i$. It is clear that sampling a direction in B^* is the best choice.

Similarly for C^1 , the best direction should be $-d_1$. Taking both d_1 and d_2 into consideration, a direction is promising only if its interaction point with Ω is the furthest to both x^1 and x^2 . It is thus the best to sample a direction in the region spanned by $-d_1$ and $-d_2$, i.e. B^* .

For $n > 2$, we have n directions with negative scores. Given the n directions, we can construct a spanned space $B = \{d = \sum_{i=1}^n \alpha_i d_i\}$. Depending on the signs of α_i 's, we have 2^N sub-regions $B^i, i = 1, \dots, 2^N$. We take B^* be the region with all negative α_i 's.

Similar to the analysis in $n = 2$, for each d_i , the point $\Omega \cap \ell_{-d_i}$ is the furthest to x^i . A direction is promising only if its interaction point with Ω is the furthest to all x^i 's. Therefore, B^* is the best region for sampling among the 2^N regions.

A direction is sampled with equal probability in Ω in random sampling. On the contrary, using negative linear combination is sampling in B^* . Therefore, we have $P_c > P_r$.

If $f(x)$ has two local minima, we have explained $P_c > P_r$. In case $f(x)$ has 3 or more local minimizers, the sampling procedure can be done as follows. Assuming we have sampled N directions, $\{d_i\}_{i=1}^N$, from which at least one local minimizer x_{last} cannot be reached. It is not wise to sample within the cones induced by local minimizers we have visited. Instead, the negative rewards associated with these directions should be used as the linear combination for sampling directions for x_{last} . Therefore, this combination is guaranteed to be more efficient to sample promising directions for x_{last} than random sampling.

APPENDIX D

To train (test) the learned policy, the Gaussian mixture functions are used (cf. Eq. 26). And we use $\Sigma_1 = \text{diag}\{1, 1\}$, $\Sigma_2 = \text{diag}\{1, 1\}$, $\mu_1 = [0, 0]^T$; $\mu_2 = [5, 5]^T$. for 2-D problem. When

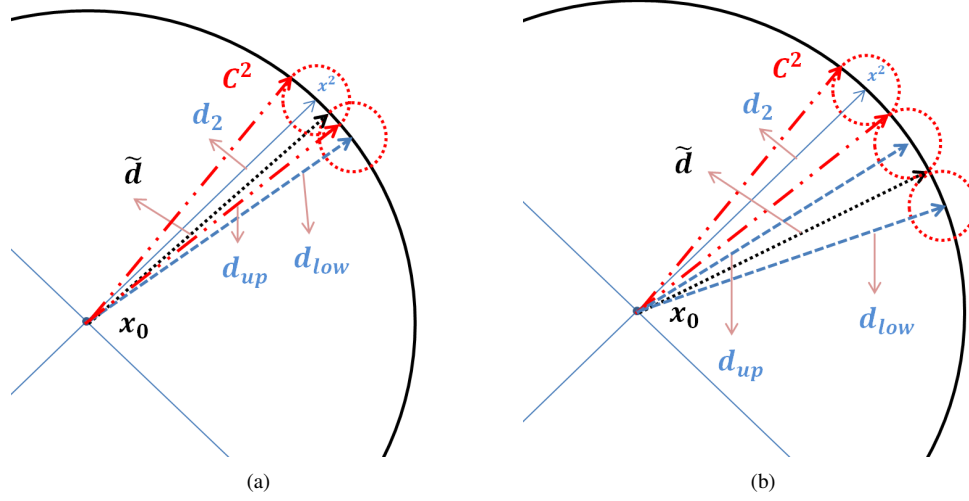


Fig. 17. Demonstration of promising direction and optimal direction. (a) shows when x^2 and $x_{\tilde{d}}$ is close to each other, d_{up} and d_{low} are close too. (b) shows when the distance between x^2 and $x_{\tilde{d}}$ is bigger than r_1 , the distance between $x_{d_{up}}$ and $x_{d_{low}}$ reaches the maximum.

testing, $\Sigma_1 = \text{diag}\{1, 1, 1, 8, 8\}$, $\Sigma_2 = \text{diag}\{1, 1, 1, 8, 8\}$, $\mu_1 = [0, 0, 0, 0, 0]^T$, $\mu_2 = [-5, -5, -5, -5, -5]^T$ for 5-D problem. When training, the following settings with different means and covariances, are applied in Table III.

- order 1-4, problem is in 2-D, $\Sigma_1 = \text{diag}\{1, 8\}$, $\Sigma_2 = \text{diag}\{1, 3\}$, $\mu_1 = [0, 0]^T$; $\mu_2 = [7, 7]^T$, $[5, 7]^T$, $[3, 7]^T$, $[4, 7]^T$ respectively;
- order 5, problem is in 5-D, $\Sigma_1 = \text{diag}\{1, 1, 1, 8, 8\}$, $\Sigma_2 = \text{diag}\{1, 1, 1, 8, 8\}$, $\mu_1 = [0, 0, 0, 0, 0]^T$, $\mu_2 = [5, 5, 5, 5, 5]^T$;
- order 6, problem is in 5-D, $\Sigma_1 = \text{diag}\{1, 1, 1, 8, 8\}$, $\Sigma_2 = \text{diag}\{1, 1, 1, 8, 8\}$, $\mu_1 = [0, 0, 0, 0, 0]^T$, $\mu_2 = [4, 4, 5, 5, 5]^T$;
- order 7, problem is in 5-D, $\Sigma_1 = \text{diag}\{1, 1, 1, 8, 8\}$, $\Sigma_2 = \text{diag}\{1, 1, 1, 8, 8\}$, $\mu_1 = [0, 0, 0, 0, 0]^T$, $\mu_2 = [3, 3, 5, 5, 5]^T$;
- order 8, problem is in 5-D, $\Sigma_1 = \text{diag}\{1, 1, 1, 1, 1\}$, $\Sigma_2 = \text{diag}\{1, 1, 1, 8, 8\}$, $\mu_1 = [0, 0, 0, 0, 0]^T$, $\mu_2 = [5, 5, 5, 5, 5]^T$;
- order 9, problem is in 5-D, $\Sigma_1 = \text{diag}\{1, 1, 1, 1, 1\}$, $\Sigma_2 = \text{diag}\{1, 1, 1, 8, 8\}$, $\mu_1 = [0, 0, 0, 0, 0]^T$, $\mu_2 = [3, 3, 5, 5, 5]^T$;